ORIGINAL ARTICLE
Polish Journal of Microbiology
2026, Vol. 75, No 1, 033-054
https://doi.org/10.33073/pjm-2026-006

# The Transcriptional Regulator Crt1 is Involved in The Pathogenic Lifestyle of *Xanthomonas campestris* pv. *campestris* B100

ANNA KORSZAŃSKA[1], PETRA LUTTER[1], VERA ORTSEIFEN[1], ALFRED PÜHLER[2] and KARSTEN NIEHAUS[1]*

[1]Department of Proteome and Metabolome Research, Faculty of Biology, Bielefeld University, Bielefeld, Germany
[2]Senior Research Group, Center for Biotechnology (CeBiTec), Bielefeld University, Bielefeld, Germany

Submitted 20 October 2025, accepted 13 December 2025, published online 31 March 2026

Abstract

The γ-proteobacterium *Xanthomonas campestris* pv. *campestris* B100 is the causal agent of black rot disease in a wide range of economically important crops. In addition, *X. campestris* pv. *campestris* is commercially relevant due to the synthesis of the exopolysaccharide xanthan. In this work, we first introduce a novel transcriptional regulator, termed Crt1, and present the effect that the deletion of the *crt1* gene exerts on growth, xanthan production, virulence, and transcriptome and proteome profiles. Differential transcriptome analysis of the deletion mutant *X. campestris* pv. *campestris* B100 Δ*crt1* compared to the wild type revealed the up-regulation of the *pilP, pilM* and *pilE* genes, which are relevant for the type 4 pilus assembly. Furthermore, increased xanthan production and upregulated transcription of genes within the *gum* cluster, which are critical for xanthan biosynthesis, were observed. Profiling of the cytosolic proteome identified increased expression of the glucosyltransferase GtrB, which is involved in LPS biosynthesis, and of a type III effector with phytase activity. Moreover, the presence of the fructose import and utilization proteins FruAB and FruK was reduced in the deletion mutant. The plant-pathogenicity assay demonstrated that the severity of the infection of the host plant tissue was higher in the case of the deletion mutant than in the wildtype strain. The regulator Crt1 modulates multiple virulence factors as well as LPS and xanthan production. In conclusion, Crt1 influences a diverse network of genes that contribute to the pathogenic lifestyle of *X. campestris* pv. *campestris*.

Keywords: *Xanthomonas campestris*, increased pathogenicity, sugar metabolism, sugar signalling, transcriptional regulator, xanthan

## Introduction

*Xanthomonas* is a genus of Gram-negative γ-proteobacterium, which poses a tremendous threat to a wide range of economically important crops and plants (Bradbury 1986; Bonas et al. 2000; Chan and Goodwin 1999; Williams 1980). The genus comprises 27 species, each with numerous highly host-plant specific pathovars (Burkholder et al. 1957; Jun et al. 2010; Parkinson et al. 2007). Moreover, more than 100 pathovars display tissue specificity upon infection of the host plant (Ryan et al. 2011). Based on recent phylo-taxonogenomic investigations, the taxonomic boundaries of the genus have been revised, revealing that several closely related genera, including *Stenotrophomonas*, *Pseudoxanthomonas,* and *Xylella*, should be reclassified under *Xanthomonas* (Bansal et al. 2023).

Belonging to the most analyzed species of the genus, *Xanthomonas campestris* pv. *campestris* is the causal agent of black rot disease in *Brassica oleracea* (*B. oleracea*), resulting in substantial losses in yield and produce quality (He and Zhang 2008; Onsando 1992; Vicente and Holub 2013). As a vascular pathogen, *X. campestris* pv. *campestris* initially colonizes the xylem vessels (Ryan et al. 2011). The most typical symptom of the black rot disease is the browning of the leaf midribs and the formation of a V-shaped lesion on the leaf with both vertices directed towards the middle vein. With the progression of the infection, the vein darkens due to the bacterial infection within the vascular system,

* Corresponding author: K. Niehaus; Department of Proteome and Metabolome Research, Faculty of Biology, Bielefeld University, Bielefeld, Germany; **e-mail: kniehaus@CeBiTec.uni-bielefeld.de**

ultimately leading to necrosis and falling of the affected leaf (Vicente and Holub, 2013).

*Xanthomonas* lives part of its life cycle saprophytically outside the host plant, for instance, freely in the soil or on plant tissue debris. The life cycle during infection can be generally divided into the epiphytic and endophytic stages. During the epiphytic stage, bacteria are introduced into the host tissue. Upon infiltrating the host plant, *X. campestris* pv. *campestris* enters the endophytic stage. Once a high population density is reached, *X. campestris* pv. *campestris* re-emerges on the leaf surface and can be transmitted to a new host (Cheng et al. 2019; Timilsina et al. 2020). At each stage, access to nutrients changes, as well as the general environmental conditions to which *X. campestris* pv. *campestris* is exposed, differ. Therefore, different regulatory cues and adaptation mechanisms must be employed depending on the current lifestyle.

The bacterial ability to successfully infect a host plant and to multiply efficiently within the invaded tissue depends on a variety of virulence factors and secretion systems that are crucial for bacterial motility, adhesion to biotic and abiotic surfaces, nutrition, stress resistance, and ultimately the suppression of the plant immune response upon infection (Büttner and Bonas, 2010; Dow et al. 2003). Despite the fact that the rich repertoire of virulence factors in *Xanthomonas* has been studied, the regulatory cues and proteins that control gene transcription in *X. campestris* pv. *campestris* still need to be investigated more thoroughly.

To identify novel putative transcriptional regulators that contribute to bacterial infection and growth *in planta,* Leßmeier (et al. 2016) conducted a pull-down approach based on DNA affinity chromatography. For this purpose, *X. campestris* pv. *campestris* cultures were grown on two different minimal media supplemented with either glucose or sucrose. The latter officiated to mimic the conditions during infection by *X. campestris* pv. *campestris*, as sucrose is the main carbon source for the pathogen *in planta*. Among the identified proteins that bound to the promoters of sucrose-related target genes, a small number were annotated as transcriptional regulators. The previously known regulators SuxR and cAMP receptor-like protein (Clp) were identified as sucrose-related. The former was confirmed to control the transcription of the sucrose transport and utilization genes in its genomic proximity (Blainvillain et al. 2007), while the latter was found bound to the putative promoter region of the *suxR* gene. This finding linked the important Quorum Sensing (QS) regulator Clp to the sucrose scavenging regulator SuxR (Leßmeier et al. 2016). Furthermore, two proteins, encoded by the previously uncharacterized genes *xccb100*_2791 and *xccb100*_2861, showed affinity for the putative promoter regions of the sucrose-related target genes. Both are predicted to be members of the LysR family of transcriptional regulators. The LysR-type transcriptional regulators (LTTRs) are the most abundant among DNA-binding proteins in prokaryotes, controlling a broad spectrum of genes, and thus are implicated in regulation of virulence, QS, motility or amino acid and carbohydrate metabolisms (Deziel et al. 2005; Hartmann et al. 2013; Heroven and Dersch 2006; Minezaki et al. 2006; O'Grady et al. 2011; Park et al. 2020; Rashid et al. 2016; Russel et al. 2004; Schulte et al. 2019). Members of this family share a highly conserved protein structure, with an N-terminal helix-turn-helix (HTH) DNA-binding domain and a C-terminal substrate-binding domain (Maddocks and Oyston, 2008). The DNA-binding putative regulator Xccb100_2791 was determined to bind promoter regions of the *suxA/suxC*, *pel3*, *pglA1*, and *suxR* genes (Leßmeier et al. 2016). It is encoded by a gene located between a putative oligosaccharide ABC exporter gene and an inner-membrane ABC exporter gene.

A recent study investigated the transcription pattern of transcriptional regulators in *X. campestris* pv. *campestris* during the nitrogen starvation induced stationary growth stage (Alkhateeb et al. 2018). The analysis revealed that three LTTRs (*ampR*, *xccb100_1534*, and *xccb100_2665*) were up-regulated in their transcription upon entry in the stationary growth stage, whereas the transcription of the *xccb100_2791* gene was down-regulated, indicating its involvement in environmental sensing (Alkhateeb et al. 2018).

In this study, we introduce XCCB100_2791 (hereafter named ***c***arbohydrate-***r***elated ***t***ranscriptional regulator Crt1, due to its affinity to sucrose-related target genes) as a novel transcriptional regulator and present a comprehensive characterization in terms of its poignant phenotypic features, virulence efficiency, repertoire of differentially expressed target genes, as well as abundance alterations within the cytosolic and membrane-bound proteome. We investigated whether and how LTTR Crt1 modulates the transcription of target genes and affects the abundance of proteins involved in the adaptation to the virulent lifestyle of *X. campestris* pv. *campestris.* For this purpose, a deletion of the *crt1* gene was constructed. The mutant was characterized with respect to phenotype and pathogenicity. Further-

more, a differential analysis was carried out between the afore-mentioned strain and the wild-type strain *Xcc* B100, both on the transcriptome and proteome level.

## Experimental

### Material and Methods

**Construction of the deletion mutant and the complemented mutant.** Unless otherwise specified, all molecular biology procedures, including chromosomal DNA purification, DNA amplification, and plasmid transformation, were performed according to standard protocols described in Green and Sambrook (2012). The *X. campestris* pv. *campestris* B100 wild-type strain was used as a parental strain for the generation of the deletion mutant and is available from the National Collection of Plant Pathogenic Bacteria (NCPPB) under the accession number NCPPB 4615 (Alkhateeb et al. 2018). The deletion mutant was constructed by disrupting the *crt1* gene utilizing the vector pk18mob*sacB* as the backbone of the cloning vector (Schäfer et al. 1994). Two fragments flanking upstream and downstream of the excision site were amplified by PCR from chromosomal DNA of *X. campestris* pv. *campestris* B100 using primers designed according to Gibson assembly cloning method (Gibson et al. 2009). All primers used for this study are listed in Supplementary Table II. Both amplified flanking regions were cloned into the pK-18mob*sacB* vector in one step Gibson assembly procedure. The cloning vector was transformed into the shuttle host, *Escherichia coli* Dh5α. The isolated cloning vector was then transformed into electrocompetent *X. campestris* pv. *campestris* B100 cells *via* electroporation. Kanamycin-resistant *X. campestris* pv. *campestris* B100 colonies that contained the integrated plasmid were selected. Bacterial colonies were transferred in parallel to selective and non-selective media. Double cross-over occurring at both flanking regions led to the directed excision of a 91 nt long sequence within the crt1 gene, causing a frameshift and disrupting the correct folding of the regulator protein. Deletion mutants were selected by colony PCR using the primers as listed in Supplementary Table II. The successful and accurate excision was validated with Sanger sequencing and MiSeq sequencing (Illumina, USA). The complemented mutant was constructed via plasmid-based complementation. The broad-host-range vector pBBR1-MCS5 carrying a gentamycin cassette was used as the backbone, and the full-length *crt1* gene, including its upstream regulatory region, was cloned into the vector using a one-step Gibson assembly procedure. The resulting plasmid was introduced into *X. campestris* pv. *campestris* B100 *Δcrt1* by electroporation, and correct integration was confirmed by Sanger sequencing of the positive clone. All sequencing approaches were carried out by the in-house sequencing core facility. The detection of SNP was carried out with analysis tool ReadXplorer2 (Hilker et al. 2016).

**Bacterial strains and growth conditions.** All bacterial strains and vectors constructed and applied in this work are listed in Supplementary Table II. All cultivations were performed in a parallel shaking flask at 180 rpm and 28°C. Pre-cultures of *X. campestris* pv. *campestris* were grown in TY rich media (5 g/l tryptone, 3 g/l yeast extract, 0.7 g/l $CaCl_2$) (Beringer 1974), intermediate and main cultures in minimal XMD media (Schatschneider et al. 2013), supplemented with 10 g/l glucose as sole carbon source and 0.6 g/l $KNO_3$ as nitrate source. Antibiotics were added to the media with respective concentrations: streptomycin 800 µg/ml, kanamycin 50 µg/ml, and gentamicin 30 µg/ml.

**Quantification of extracellular xanthan in the culture media.** Xanthan quantification was performed according to Palaniraj et al. (2011). For this purpose, *X. campestris* pv. *campestris* main cultures were grown in minimal XMD media as described above and harvested after 72 h of cultivation. Cells were diluted 1:8 (v/v) in pre-cooled water and subsequently centrifuged for 1 h at 12,500 rpm and 4°C. Afterwards, the supernatant was separated thoroughly from the pellet and added to pre-cooled absolute isopropanol 1:3 v/v. After 30 min of incubation on ice, the sample was centrifuged for 90 min at 9,000 rpm at 4°C. The resulting supernatant was carefully discarded, and the xanthan pellet was dried for 72 h at 60°C and subsequently weighed. For each strain, 5 biological replicates have been considered. For the assessment of statistical significance, an equal-variance t-test was performed.

**Rheometric measurements of xanthan harvested from culture media.** Viscosity of xanthan harvested from *X. campestris* pv. *campestris* cultures was measured utilizing a rotational viscometer (Physica MCR 101, Anton Paar, Austria). For this purpose, dried EPS was diluted to 1% w/v in sterile water. For each measurement, 1.5 ml of the sample was placed on the stationary plate. The measurements were carried out at room temperature, and all calculations were performed with RheoPlus Rheometer Software (Anton

Table II
Effect of the *crt1* deletion on the cytosolic and membrane-bound proteome of *X. campestris pv. campestris* during early stationary growth stage.

| Locus | Gene name | Function | Abundance ratio | p-Value | Unique peptides |
|---|---|---|---|---|---|
| **Up-regulated proteins** | | | | | |
| XCCB100_1291 | *gtrB* | putative bactoprenol glucosyltransferase | 5.92 | 1.00E-17 | 3 |
| XCCB100_3258 | | conserved hypothetical protein | 3.67 | 1.30E-05 | 4 |
| XCCB100_3905 | | putative carboxypeptidase | 3.50 | 4.47E-07 | 3 |
| XCCB100_2818 | *int* | phage-related integrase | 3.19 | 1.05E-04 | 3 |
| XCCB100_1799 | *rpfN* | carbohydrate-selective porin | 3.08 | 1.00E-17 | 20 |
| XCCB100_3640 | | conserved hypothetical protein | 3.08 | 1.00E-17 | 4 |
| XCCB100_1801 | *fruK* | 1-phosphofructokinase | 2.89 | 1.00E-17 | 7 |
| XCCB100_1802 | *fruB* | PTS fructose porter | 2.71 | 1.00E-17 | 35 |
| XCCB100_2558 | *ftsB* | septum formation initiator protein FtsB | 2.41 | 3.35E-11 | 3 |
| XCCB100_2909 | | conserved hypothetical protein | 2.19 | 6.21E-06 | 3 |
| XCCB100_1450 | | pirin-related protein | 2.14 | 5.65E-09 | 7 |
| XCCB100_0445 | | hypothetical protein | 2.08 | 1.00E-17 | 4 |
| XCCB100_2092 | | transcriptional regulator; Crp/Fnr family | 2.02 | 2.26E-07 | 3 |
| XCCB100_1788 | *phy* | putative exported phytase | 1.96 | 8.66E-12 | 3 |
| XCCB100_0128 | | TonB-dependent outer membrane receptor precursor | 1.95 | 4.39E-12 | 18 |
| XCCB100_1697 | *aglA1* | alpha-glucosidase | 1.95 | 1.81E-08 | 11 |
| XCCB100_1807 | *gdh* | glutamate dehydrogenase | 1.87 | 1.00E-17 | 124 |
| XCCB100_1800 | *fruA* | PTS fructose porter | 1.82 | 1.00E-17 | 12 |
| XCCB100_1894 | | conserved hypothetical protein | 1.77 | 2.80E-07 | 7 |
| XCCB100_1761 | | conserved hypothetical protein | 1.74 | 6.40E-12 | 3 |
| **Down-regulated proteins** | | | | | |
| XCCB100_0308 | *agxT* | aminotransferase | -2.54 | 1.66E-03 | 4 |
| XCCB100_3852 | | putative aromatic ring-opening dioxygenase | -2.31 | 2.09E-04 | 3 |
| XCCB100_0796 | | putative nuclease / phosphatase | -2.31 | 3.84E-04 | 3 |
| XCCB100_0846 | *tctE* | two-component system sensor histidine kinase | -2.28 | 2.85E-04 | 5 |
| XCCB100_2019 | | short chain dehydrogenase | -2.22 | 5.37E-05 | 6 |
| XCCB100_3906 | | putative transcriptional regulator; LysR family | -2.21 | 1.93E-13 | 6 |
| XCCB100_4189 | | conserved hypothetical protein | -2.17 | 7.94E-12 | 3 |
| XCCB100_1528 | | ABC transporter permease and ATP-binding protein | -2.09 | 5.28E-03 | 5 |
| XCCB100_1398 | | DJ-1/PfpI family protein | -2.09 | 1.12E-07 | 8 |

| | | | | | |
|---|---|---|---|---|---|
| XCCB100_2784 | | conserved hypothetical protein | -2.08 | 2.49E-08 | 7 |
| XCCB100_3277 | *hsdR2* | Type I site-specific deoxyribonuclease (restriction subunit) | -1.96 | 7.02E-04 | 8 |
| XCCB100_2866 | *asnB2* | asparagine synthase (glutamine-hydrolysing) | -1.95 | 1.68E-06 | 10 |
| XCCB100_0546 | | conserved hypothetical protein | -1.85 | 3.77E-04 | 3 |
| XCCB100_2526 | *thiD* | phosphomethylpyrimidine kinase | -1.83 | 9.26E-04 | 6 |
| XCCB100_2607 | *rpfS* | DSF-sensing histidine kinase/response regulator hybrid | -1.79 | 3.06E-02 | 3 |
| XCCB100_0601 | | membrane-located putative protein phosphatase | -1.76 | 4.57E-04 | 5 |
| XCCB100_1293 | *asmA* | AsmA family membrane protein | -1.64 | 2.84E-03 | 7 |
| XCCB100_2313 | | NDP-hexulose epimerase | -1.62 | 1.40E-02 | 3 |
| XCCB100_4124 | *birA* | bifunctional biotin repressor / co-repressor biosynthesis enzyme | -1.58 | 3.02E-02 | 3 |
| XCCB100_2292 | | short chain dehydrogenase | -1.56 | 1.98E-04 | 6 |

Proteins with most significant abundance fold-change under deletion of crt1 gene as compared to the wild-type strain *X. campestris pv. campestris* B100; Abundance ratio represents the fold-change [$\log_2$] measured for replicates of deletion mutant relative to replicates of wild-type; Abundance ratio p-value has been calculated with significance background-based, nested ANOVA test, with n = 3; unique peptides describe number of peptides that occur exclusively in the given target protein were employed for its identification.

Paar, Austria). For each strain, 4 biological replicates have been considered. To investigate the statistical significance of the obtained results, a paired two-sample t-test was performed.

**Transcriptome analysis.** Three independent biological replicates of each strain were cultivated in minimal XMD medium with 10 g/l glucose and harvested at the early stationary growth stage, with an $OD_{600}$ nm of 1.8. Cultivation of *X. campestris* pv. *campestris* in sucrose leads to overproduction of EPS during the early stationary stage, hence preventing to obtain material of high quality and purification grade without distorting the results of the whole-genome analysis.

**RNA Isolation.** For the purpose of isolation of total RNA, cells were harvested by centrifugation at 14,000 rpm for 4 minutes. The resulting cell pellet was frozen immediately in liquid nitrogen and stored at -80°C until further treatment. Frozen cell pellets were suspended carefully in 2 ml DNA/RNA Shield provided with the Quick RNA Miniprep Kit (ZymoResearch, USA), and 750 µl of the suspension was transferred to Lysing Matrix Tubes (MP Biomedical, USA), containing ceramic and glass beads, for homogenization. Cells were disrupted by the Ribolyzer (Hybaid, Germany) thrice for 40 sec at speed setting 6.5, and 2-min cooling on ice in between the homogenization steps. After the centrifugation for 5 min at 4°C and 13,500 rpm, supernatant was transferred into new RNAse-free reaction tubes. All subsequent steps of RNA isolation and DNA digestion were carried out with Quick RNA Miniprep Kit and RNA Clean & Concentrator (ZymoResearch, USA) according to the manufacturer's protocol. To verify complete removal of residual DNA, PCR with primers binding to multiple genomic regions was carried out. Quantity of the RNA was measured with a NanoDrop 1000 ND-1000 spectrophotometer (Thermo Fisher, USA).

**Synthesis and fluorescent labelling of the cDNA.** All the subsequent experimental procedures, including cDNA synthesis, labelling of cDNA, hybridization, and washing of microarrays were performed according to the protocol Two-Color Microarray-Based Prokaryote Analysis FairPlay III Labeling (Agilent Technologies, USA). Any adjustments to the afore-mentioned protocol are described below. To synthesize cDNA for each strain, three biological replicates were pooled in equal amounts to 5 µg of total RNA, and AffinityScript HC Reverse Transcriptase and aminoallyl dUTPs were used. Purified cDNA was labeled with Cy3- or Cy5-N-hydroxysuccinimidyl ester mono-reactive dyes (GE Healthcare, UK). Subsequent quantification of labelled cDNA, as well as specific activity of mono-reactive dyes, was performed with NanoDrop ND-1000 spectrophotometer (Thermo Fisher, USA) with the method ssDNA-33. Only samples with specific activity of at least 40 pmol of mono-reactive dye per µg of cDNA were considered for the subsequent hybridization.

**Whole genome oligonucleotide microarrays.** For the purpose of this study, custom whole-genome oli-

gonucleotide microarrays representing the coding sequence of *X. campestris* pv. *campestris* B100 were designed with Agilent eArray and ordered in the 8x15K format (both Agilent Technologies, USA). Each array consists of 4,679 features representing genes and putative small RNAs of *Xanthomonas campestris* pv. *campestris* B100. The complete design and dataset of the microarray have been deposited at EMBL ArrayExpress Archive for Functional Genomics, accession number E-MTAB-12383. For each microarray the mix was prepared with 330 ng of Cy3-labeled cDNA, 330 ng of Cy5-labeled cDNA, and 11 µl gene expression blocking agent. The cDNA blocking mix was filled up to 55 µl with $H_20$ and joined with 55 µl Hi-RPM hybridization buffer. The quantities were adjusted to fit the 8x15K format of the array. For each microarray, 100 µl of the hybridization mix was used. To reduce artefact formation, the washing procedure was modified by increasing the number of wash cycles (both 5 minutes in buffer 1 and 1 minute in buffer 2, as described in the manufacturer's protocol). All procedures, reagents, and equipment for microarray hybridization and scanning were ordered and used as described in the manufacturer's protocol referenced above.

**Feature extraction and data analysis.** Feature extraction was performed according to the manufacturer's protocol with the Agilent Feature Extraction Software (Agilent Technologies, USA), and the obtained data were further analysed with the web-based software EMMA2 (Dondrup et al. 2009). For this study, data from two arrays, resulting from a two-colour dye-swap approach, were combined to obtain more reliable results. The data were normalized using the LOWESS method, and a subsequent one-sample Holm t-test was performed. Transcripts with the logarithmic signal intensities (A-value) ≥ 8.0, mean values of transcriptome fold-change [$\log_2$] (M-value) ≥ 1 or ≤ -1, and the p-value ≤ 0.05, were considered as significantly differentially regulated.

**Proteome analysis. Extraction of proteins from *X. campestris* pv. *campestris* cell pellets, tryptic digestion, and purification.** In order to investigate the cytosolic proteome, both *X. campestris* pv. *campestris* strains were cultivated as described above for the transcriptome analysis. Sample preparation, tryptic digestion, and SEP Pak purification were carried out according to Wang [et al. 2005] and Russell [et al. 2001]. *X. campestris* pv. *campestris* cells were first diluted 1:2 v/v in 0.9% NaCl and promptly centrifuged at 4°C and 13,500 rpm for 2 minutes. Afterwards, the supernatant was completely discarded and the remaining pellets, consisting of cytosolic and periplasmic proteins, were frozen in liquid nitrogen. Frozen cell pellets were lyophilized in order to dispose of the water molecules that would interfere with the sample purification and final measurements. To each lyophilized sample, 100 µl of 100mM ammonium bicarbonate (Ambic), 100 µl 2,2,2-trifluoroethanol (TFE), and 5 µl 200 mM Tris (2-carboxyethyl) phosphine (TCEP) were added. During the incubation at 60°C for 60 minutes, samples were occasionally inverted. Subsequently, 20 µl of 400 mM chloroacetamide was added to each sample, and the samples were further incubated at room temperature in the dark for 90 minutes. Afterwards, 5 µl of TCEP was added to each sample, and the samples were incubated at room temperature for 60 minutes. In the next step, 437 µl Ambic and 437 µl $ddH_2O$ were added. Finally, 2 µl of 1 µg $µl^{-1}$, Trypsin Gold (Mass Spectrometry Grade, Promega, USA) was added and the samples were incubated overnight at room temperature.

After digestion, samples were purified using Sep-Pak C18 Columns (Waters Corporation, USA) as described earlier (Droste et al. 2020). Afterwards, the eluted samples were dried in a vacufuge concentrator (Eppendorf, Germany) and rehydrated with 12 µl Solution A (98% Acetonitril, 2% $ddH_20$, 0.01% TFA). Rehydrated samples were centrifuged at 13,500 rpm for 2 minutes. Protein concentration and purity of the samples were assessed with NanoDrop 2000/2000c (Thermo Fisher, USA) at the wavelength of 280 nm.

**Mass spectrometry measurements and data analysis.** Mass spectrometry was performed on a Q Exactive mass spectrometer (Thermo Fisher, USA). The peptides were separated on a 25 cm steel column Acclaim™ PepMap™ C18-LC-column with a particle size of 2 µm and a diameter of 75 µm (Thermo Fisher, USA). For data analysis, ms spectra were searched with SEQUEST against the target-decoy protein sequence database of *X. campestris* pv. *campestris* B100. Protein abundances were determined with the Proteome Discoverer 2.3 (Thermo Fisher, USA). Only unique peptides were used for the quantification. An oxidation of methionine (15.99 Da) was allowed up to three times per peptide. As a static modification, a carbamidomethylation of cysteine (57.02 Da) and the dynamic modification of the N-terminus with an acetylation (42.01 Da) were allowed. The mass spectrometry proteomics data have been deposited in the MassIVE via the PRIDE partner depository with the data set identifier (Identifier for Review Process: Dataset MSV000090790).

**Plant material and plant inoculations.** *Brassica oleracea* 'express' cultivar (Quedlinburger Saatgut, Germany) was used as a host plant for *X. campestris* pv. *campestris* strains. All plants were grown on soil in a humidified chamber at 23°C in incandescent light with a 16 h light/ 8 h dark cycle. *X. campestris* pv. *campestris* strains were grown overnight at 28°C on agar plates in TY rich medium supplemented with antibiotic streptomycin 800 µg/ml. The leaves of 4-week-old seedlings were inoculated by infiltrating a single colony of the bacterial strain using a sterile needle. At least 11 plants were infiltrated by either of the *X. campestris* pv. *campestris* strains. Additionally, mock inoculation was performed on 5 plants by infiltration with a sterile syringe only in order to exclude mechanical stress upon leaf tissue as the potential cause of occurring disease symptoms. The infection symptoms were observed and photographed every 48 h after inoculation. Both lesion area and entire leaf area at 10 dpi were quantified using FIJI software (Schindelin et al. 2012). Disease was rated by the percentage of the entire leaf area affected by the bacterial strain. For each strain, ≥ 11 replicates have been assessed, and a two-tailed t-test ($p < 0.01$) was performed for both sample groups.

## Results and Discussion

**Bioinformatic analysis of the *crt1* gene and therein encoded transcriptional regulator Crt1.** Gene *crt1* is located at the position 3207118 to 3208017 in the genome of *X. campestris* pv. *campestris* B100 (Supplementary Fig. 1). It is proposed to be organized as a gene downstream of the gene *msbA*4 within a single

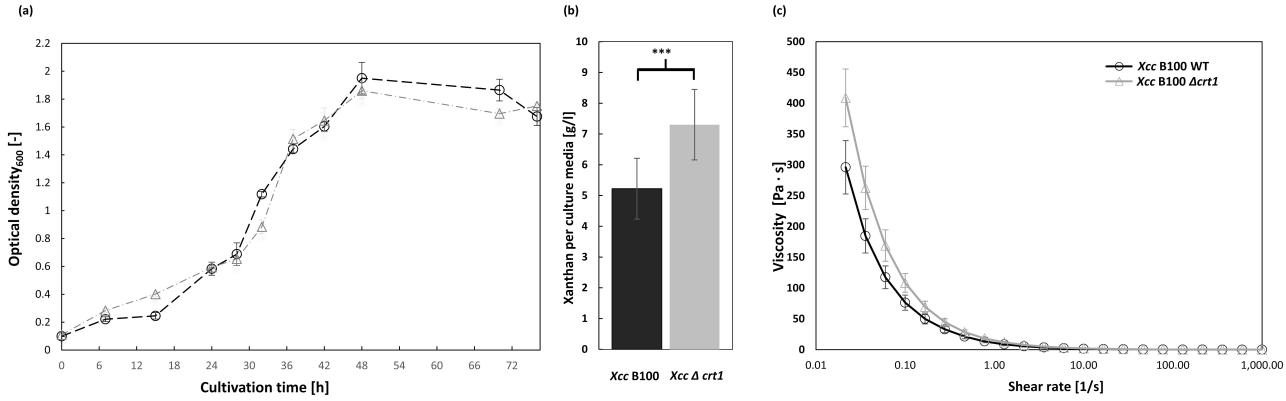


Fig. 1. Phenotype characterization of the deletion mutant *Xanthomonas campestris* pv. campestris B100 Δ*crt*1 compared to the wild-type strain *Xanthomonas campestris* pv. campestris B100.

a) Growth behaviour of the wild-type (○) and the deletion mutant (Δ) strains cultivated in XMD minimal medium with 10 g/l glucose as sole carbon source; b) xanthan production was measured after 72 h of cultivation; xanthan was precipitated with isopropanol, dried and weighted relative to culture media; n≥ 5 biological replicates were investigated; two-tailed t-test resulted in significant p-value of 0.027 (***); viscosity of xanthan was assessed for both strains; xanthan was harvested after 72 h of cultivation, isolated and dried; all measurements were performed with 1% w/v xanthan with rheometer at room temperature; n = 4 biological replicates were investigated for each strain.

operon, based on RNA sequencing data, partially presented in the genome-wide study of transcription start sites (Alkhateeb et al. 2016). The genes in its immediate vicinity encode a putative lipooligosaccharide ABC exporter and an inner membrane ABC efflux protein (*msbA4* and *xccb100_2792*, respectively), as shown in Supplementary Fig. 2. Investigation of the coding sequence of the ORF *xccb100_2791* provided the first insight into the putative role of the newly identified regulator Crt1. The gene product Xccb100_2791 comprises 299 amino acid residues with a predicted molecular mass of 32 kDa. It contains two protein domains, a winged HTH DNA-binding domain (amino acids 8 to 66), and a LysR substrate-binding domain (amino acids 93 to 298). A more detailed analysis based on SWISS-MODEL revealed potential homo-dimer and homo-tetramer formation of the Crt1 protein, similar to that of another LysR-family regulator, OxyR (Bertoni et al. 2017; Guex et al. 2009; Waterhouse et al. 2018).

**Construction of the putative transcriptional regulator disruption mutant *X. campestris* pv. *campestris* B100 *Δcrt1*.** In order to confirm Crt1 as a transcriptional regulator and to gain a first insight into the network of genes under its control, the *crt1* gene in

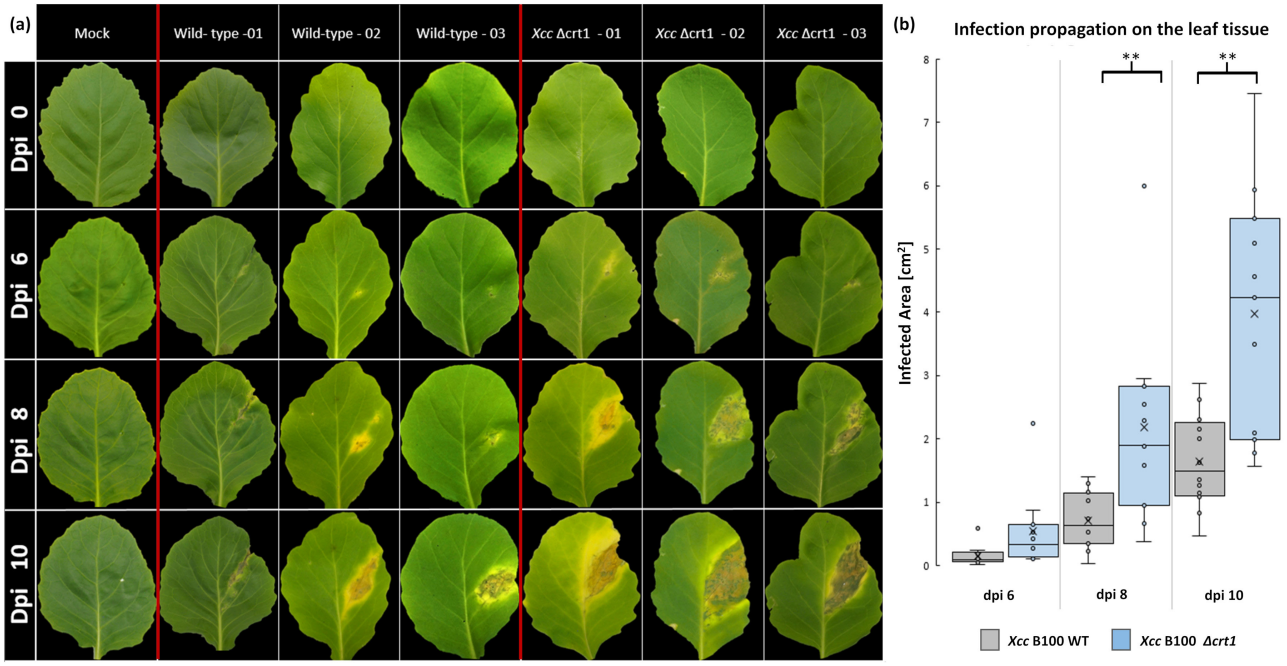


Fig. 2. Bacterial virulence against host plant *Brassica oleracea*.

a) Leaf lesions in *Brassica oleracea* caused 6,8, and 10 dpi by infection with the *X. campestris* pv. campestris B100 wild-type (WT), deletion mutant strain *X. campestris* pv. campestris B100 *Δcrt1,* and a mock sample; inoculation was conducted with a sterile syringe, infection progress was documented at 6,8, and 10 days post inoculation; a representative set of leaves was chosen for the depiction of symptom propagation; b) analysis of the lesion area of the plants infected with either wild-type or deletion mutant strain, measured at 0, 6, 8, and 10 days post inoculation; depicted are calculated mean values for each condition; statistical relevance was confirmed by t-test (Supplementary Table I), for each bacterial strain n ≥11 samples were considered.

the wildtype strain *X. campestris* pv. *campestris* B100 was disrupted by a non-in-frame deletion. For this purpose, regions flanking the deletion site upstream and downstream were cloned into the pK18*mobsacB* vector, and the region of interest was excised from the genome via double cross-over. Successful excision of the fragment within the *crt1* coding sequence was confirmed by whole-genome sequencing, which was carried out to identify any single-nucleotide polymorphism (SNP) divergence between the wildtype strain *X. campestris* pv. *campestris* B100 and the novel deletion mutant *X. campestris* pv. *campestris* B100 *Δcrt1*. In addition to confirming the directed deletion within the *crt1* coding sequence, two SNPs were determined within the coding sequences of *fhuA* and *nuoN*. In both cases, the SNPs result in an amino acid exchange: however, in-depth *in silico* analysis showed no effect on the structure or functionality of the proteins encoded by *fhuA* and *nuoN*. For this purpose, the open-source toolboxes within RaptorX and SWISS-MODEL were used (Bertoni et al. 2017; Guex et al. 2009; Wang et al. 2017b; Wang et al. 2018; Waterhouse et al. 2018; Xu et al. 2021). Furthermore, both genes, *fhuA* and *nuoN,* and the proteins encoded by them were not identified in the differential analysis of the transcriptome and proteome, respectively, among those with the most significant fold changes.

**Phenotypical characterization of the *crt1* deletion mutant. Disruption of the *crt1* gene does not affect growth behavior, yet results in significantly increased xanthan production.** To characterize the phenotype of the obtained deletion mutant *X. campestris* pv. *campestris* B100 Δ*crt1*, first, its growth was compared with that of the ancestral wild-type strain in parallel shaking flask cultivation with minimal XMD medium supplemented with 10 g/l glucose as the sole carbon source. Disruption of the *crt1* gene did not influence the growth, as shown in Fig. 1a. Thus, the transcriptional regulator is not implied to control the growth of the *X. campestris* pv. *campestris* at any growth stage under laboratory conditions in minimal medium. However, the measured xanthan output was increased by 39.8% in the *X. campestris* pv. *campestris* B100 *Δcrt1* culture to 7.3 g/l culture compared to 5.22 g/l of EPS measured for wild-type *X. campestris* pv. *campestris* B100 (Fig. 1b).

The significance of the measured difference was confirmed by an equal-variance t-test, yielding a two-

tailed p-value of 0.011. For each condition, at least 5 biological replicates were considered. Similarly, the detected viscosity of the mutant strain was significantly higher than that of the wild-type strain (Fig. 1c). For each strain, xanthan obtained from four biological replicates has been used, and the statistical analysis using a paired two-sample, two-tailed t-test for means led to a significant p-value of 0.027. Furthermore, EPS quantification was carried out for wild-type, deletion mutant and complemented mutant strains *X. campestris* pv. *campestris* B100 *Δcrt1::crt1*. The xanthan output was measured as 3.92 g/l, 4.99 g/l, and 4.06 g/l of the culture, respectively. The significance between the measurements of the deletion mutant, and both wild-type and complemented mutant was confirmed with a two-tailed t-test with p-values of 0.028 and 0.035, respectively. Two-tailed t-test demonstrated no statistical significance between wild-type *X. campestris* pv. *campestris* B100 and the complemented mutant strain (Supplementary Fig. 3).

*X. campestris* pv. *campestris* synthesises xanthan under nitrogen limitation during the stationary growth stage, thus the increase in the EPS output has no effect on the biomass formation during exponential bacterial growth. The role of EPS xanthan has been suggested to be beneficial for *Xanthomonas* during the colonization of host plant tissue (Vojnov et al. 2000; Alvarez et al. 2000; Yun et al. 2006). Other studies have suggested that xanthan biosynthesis is modulated by components of Quorum Sensing (Dow et al. 2003; Crossman and

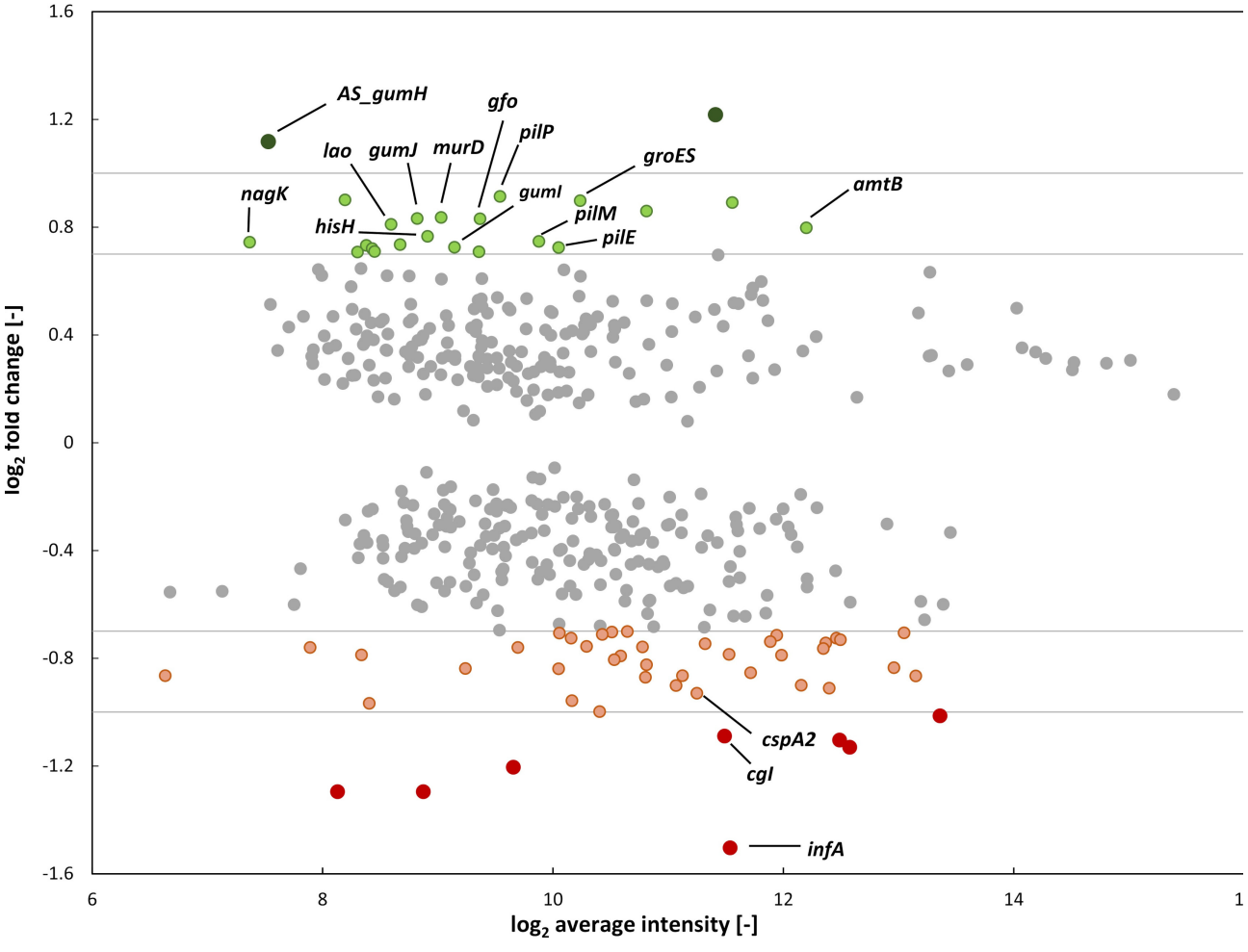


Fig. 3. Genome-wide differential transcriptional analysis of the deletion mutant *Xanthomonas campestris* pv. campestris B100 *Δcrt1* compared to the wild-type strain.

Ratio/intensity plot obtained from whole genome microarrays of the strain *X. campestris* pv. campestris B100 *Δcrt1* compared to the wild-type strain *X. campestris* pv. campestris B100; cultivation was performed in the minimal XMD medium with 10 g/l glucose as a sole carbon source; cells were harvested at an early stationary growth stage at an $oD_{600}$ nm of 1.8; shown are only targets with confidence level greater than 95%; green and red dots represent target genes with increased and decreased, respectively, transcript levels in the mutant strain *X. campestris* pv. campestris B100 *Δcrt1*; genes with transcription unaffected by the deletion of *crt1* gene are represented by grey dots; annotated target genes with highest fold-change compared to the wild-type strain marked by gene name.

Table I
Effect of the *crt1* deletion on *X. campestris pv. campestris* gene expression.

| Locus | Gene name | Annotated gene product | M-value | A-value | p-Value |
|---|---|---|---|---|---|
| **Up-regulated genes** | | | | | |
| XCCB100_2325 | | putative filamentous hemagglutinin-related protein | 1.22 | 11.4 | 7.42E-04 |
| *AS*_XCCB100_1718 | | antisense transcript *gumH* | 1.12 | 7.5 | 3.49E-03 |
| XCCB100_0957 | *pilP* | type IV pilus assembly protein | 0.91 | 9.5 | 9.00E-04 |
| XCCB100_0907 | | putative cytochrome c551 | 0.90 | 8.2 | 4.92E-03 |
| XCCB100_0552 | *groES* | 10 kDa chaperonin | 0.90 | 10.2 | 1.99E-03 |
| XCCB100_0905 | | putative exported protein | 0.89 | 11.6 | 2.65E-03 |
| XCCB100_3396 | | putative exported enzyme | 0.86 | 10.8 | 1.23E-09 |
| XCCB100_1423 | *murD* | UDP-N-acetylmuramoylalanine-D-glutamate ligase | 0.84 | 9.0 | 3.95E-03 |
| XCCB100_1720 | *gumJ* | xanthan repeating unit exporter | 0.83 | 8.8 | 3.25E-02 |
| XCCB100_3538 | *gfo* | exported glucose-fructose oxidoreductase | 0.83 | 9.4 | 3.07E-02 |
| XCCB100_0906 | *lao* | L-amino-acid oxidase | 0.81 | 8.6 | 8.41E-03 |
| XCCB100_0207 | *amtB* | ammonium transporter | 0.80 | 12.2 | 6.28E-04 |
| XCCB100_2099 | *hisH* | glutamine amidotransferase | 0.77 | 8.9 | 7.83E-03 |
| XCCB100_0954 | *pilM* | type IV pilus assembly protein | 0.75 | 9.9 | 4.70E-03 |
| XCCB100_1209 | *glk2* | glucokinase | 0.74 | 7.4 | 1.86E-02 |
| XCCB100_1615 | | conserved hypothetical protein | 0.74 | 8.7 | 1.76E-02 |
| XCCB100_2311 | | hexose O-acetyltransferase | 0.73 | 8.4 | 2.52E-02 |
| XCCB100_rna061 | | putative regulatory sRNA | 0.73 | 19.7 | 1.86E-04 |
| XCCB100_1719 | *gumI* | mannosyltransferase | 0.73 | 9.1 | 1.21E-02 |
| XCCB100_1672 | *pilE* | type IV pilus assembly protein PilE | 0.72 | 10.0 | 6.89E-03 |
| **Down-regulated genes** | | | | | |
| XCCB100_2267 | *infA* | translation initiation factor IF-1 | -1.50 | 11.5 | 1.11E-04 |
| XCCB100_2352 | | hypothetical protein | -1.30 | 8.9 | 7.20E-04 |
| XCCB100_1776 | | hypothetical protein | -1.30 | 8.1 | 4.39E-02 |
| XCCB100_1297 | | homoserine O-acetyltransferase-like enzyme | -1.20 | 9.7 | 6.91E-06 |
| XCCB100_2980 | | conserved hypothetical protein | -1.13 | 12.6 | 7.39E-09 |
| XCCB100_3868 | | conserved hypothetical protein | -1.10 | 12.5 | 3.37E-04 |
| XCCB100_1298 | *cgl* | cystathionine gamma-lyase | -1.09 | 11.5 | 1.50E-07 |
| XCCB100_4110 | | hypothetical protein | -1.01 | 13.4 | 3.72E-03 |
| XCCB100_3996 | | conserved hypothetical protein | -1.00 | 10.4 | 1.31E-08 |
| XCCB100_2290 | | TonB-dependent outer membrane receptor precursor | -0.97 | 8.4 | 2.37E-03 |
| XCCB100_rna193 | | putative regulatory RNA | -0.96 | 10.2 | 2.16E-03 |
| XCCB100_3017 | *cspA2* | cold shock protein | -0.93 | 11.2 | 3.27E-06 |
| XCCB100_3810 | | putative secreted protein | -0.91 | 12.4 | 8.14E-03 |
| XCCB100_1741 | | conserved hypothetical protein | -0.90 | 11.1 | 1.29E-02 |
| XCCB100_3869 | | putative manganese-containing catalase | -0.90 | 12.2 | 2.48E-03 |
| XCCB100_3892 | | conserved hypothetical protein | -0.87 | 10.8 | 8.28E-03 |
| XCCB100_2320 | | conserved hypothetical protein | -0.87 | 13.1 | 7.39E-03 |
| XCCB100_2291 | | hypothetical protein | -0.86 | 11.1 | 7.85E-03 |
| XCCB100_1773 | | hypothetical protein predicted | -0.86 | 6.6 | 1.02E-04 |
| XCCB100_3966 | | putative exported protein | -0.85 | 11.7 | 2.14E-10 |

Target genes with most fold-change of transcription under deletion of *crt1* gene as compared to the wild-type strain *X. campestris* pv. *campestris* B100; M-value represents the fold-change [$\log_2$] of transcript in mutant strain compared to wild-type strain; A-value denotes the intensity of the given signal; p-value has been calculated with significance test with Holm method.

Dow 2004). In light of these findings, the increased xanthan production in the mutant strain may improve the protection of *X. campestris* pv. *campestris* against adverse environmental conditions, including plant defense mechanisms.

**Investigation of pathogen–plant interactions between *X. campestris* pv. *campestris* and *Brassica oleracea* demonstrate more rapid infection propagation under deletion of the transcriptional regulator Crt1.** The putative transcriptional regulator Crt1 was identified in an approach to screen for sucrose-related regulatory proteins and showed affinity for the promoter regions of target genes differentially expressed under sucrose supplementation of the growth media (Leßmeier et al. 2016). As sucrose is abundant in the plant tissues, it serves as a major carbon source for the *Xanthomonas* scavenged from the host cell. Proteins that bind to the promoters of the sucrose-related target genes are therefore implied to play a role in the pathogenic behaviour of *X. campestris* pv. *campestris*.

To investigate the influence Crt1 exerts on bacterial virulence regulation, we conducted *in planta* experiments. For this purpose, virulence assays were employed to test the effect of both the wildtype strain *X. campestris* pv. *campestris* B100 and the deletion mutant *X. campestris* pv. *campestris* B100 Δ*crt1* on the host plant *Brassica oleracea* (*B. oleracea*). Mock inoculation was performed to exclude mechanical stress on the leaf material as a potential cause of the observed symptoms. Six days post inoculation (dpi) of bacterial cells, the first disease symptoms on *B. oleracea* leaves were noticeably visible on host plants inoculated with either strain, whereas no disease hallmarks were noticed on plant material with only a mock inoculation (Fig. 2a). The average lesion area caused by the inoculation of cabbage leaves with the wild-type strain was 0.15, 0.71 and 1.64 [$cm^2$] at 6, 8 and 10 dpi, respectively (Fig. 2b). Infection with the deletion mutant strain *X. campestris* pv. *campestris* B100 Δ*crt1* resulted in a remarkable increase in lesion area with a calculated value of 0.54 [$cm^2$] at 6 dpi, 2.18 [$cm^2$] at 8 dpi, and 3.97 [$cm^2$] at 10 dpi. To statistically evaluate these findings, a two-tailed t-test with $n \geq 11$ was conducted for each condition at each measurement time point (Supplementary Table I and Fig. 2). The analysis yielded p-values of 0.06 at dpi 6, 0.005 at dpi 8, and 0.0027 at dpi 10. These data show that deletion of the crt1 gene led to a distinct, statistically significant increase in the virulence of *X. campestris* pv. *campestris* against *B. oleracea*. Investigation of infection propagation was additionally performed for both of the aforementioned strains and the complemented mutant *X. campestris* pv. *campestris* B100 *Δcrt1::crt1*. The latter demonstrated significantly decreased infection efficiency compared to the deletion mutant *X. campestris* pv. *campestris* B100 *Δcrt1*. The calculated mean of the infection area was nearly equal to the mean value for leaves infected with wild-type colonies (Supplementary Fig. 4 and Supplementary Table III).

Strikingly, the deletion of the *crt1* did not affect the growth of *X. campestris* pv. *campestris in vitro*, however, it greatly affected the infection propagation within the host plant tissue compared to the wild-type strain. Since *in silico* analysis predicted that Crt1 contains an HTH DNA-binding domain, we decided to investigate the regulatory network of the regulator Crt1 in more detail.

**Microarray-based investigation of the transcriptional regulatory network of the regulator Crt1.** To investigate the effect of the deletion of the transcriptional regulator gene *crt1* on the transcriptome of *X. campestris* pv. *campestris*, comparative genome-wide analysis was conducted with microarrays. For this purpose, three independent biological replicates of each strain were cultivated in minimal XMD medium with 10 g/l glucose and harvested at the early stationary growth stage with an $OD_{600}$ nm of 1.8.

For this study, only target genes with p-value ≤0.05 were considered for further analysis (Fig. 3). Statistical analysis of the whole transcriptome resulted in the identification of 11 differentially expressed genes with M-values ≥ 1 or ≤ -1, manifesting that the novel transcriptional regulator Crt1 exerts its regulatory function merely as an adaptation under particular conditions. Upon deletion of *crt1*, only two target genes showed increased transcription (M-values ≥ 1). Significant upregulation of transcription was observed for the antisense transcript within the coding sequence of *gumH*. Furthermore, among 20 targets with the highest up-regulation *gumI* and *gumJ* were identified (Table I). This finding coincides with the examined phenotype of the deletion mutant, which showed significantly increased production of the EPS xanthan (Fig. 1b), and indicates that modulation of transcription of genes downstream of the primary TSS *gumH* significantly impacts xanthan biosynthesis, possibly serving as a bottleneck in xanthan generation.

Noteworthy is moderate upregulation of transcription of several motility-related genes coding for type IV pilus assembly proteins *pilP*, *pilM*, and *pilE*, with M-values of 0.91, 0.75, and 0.72, respectively. *pilP* and

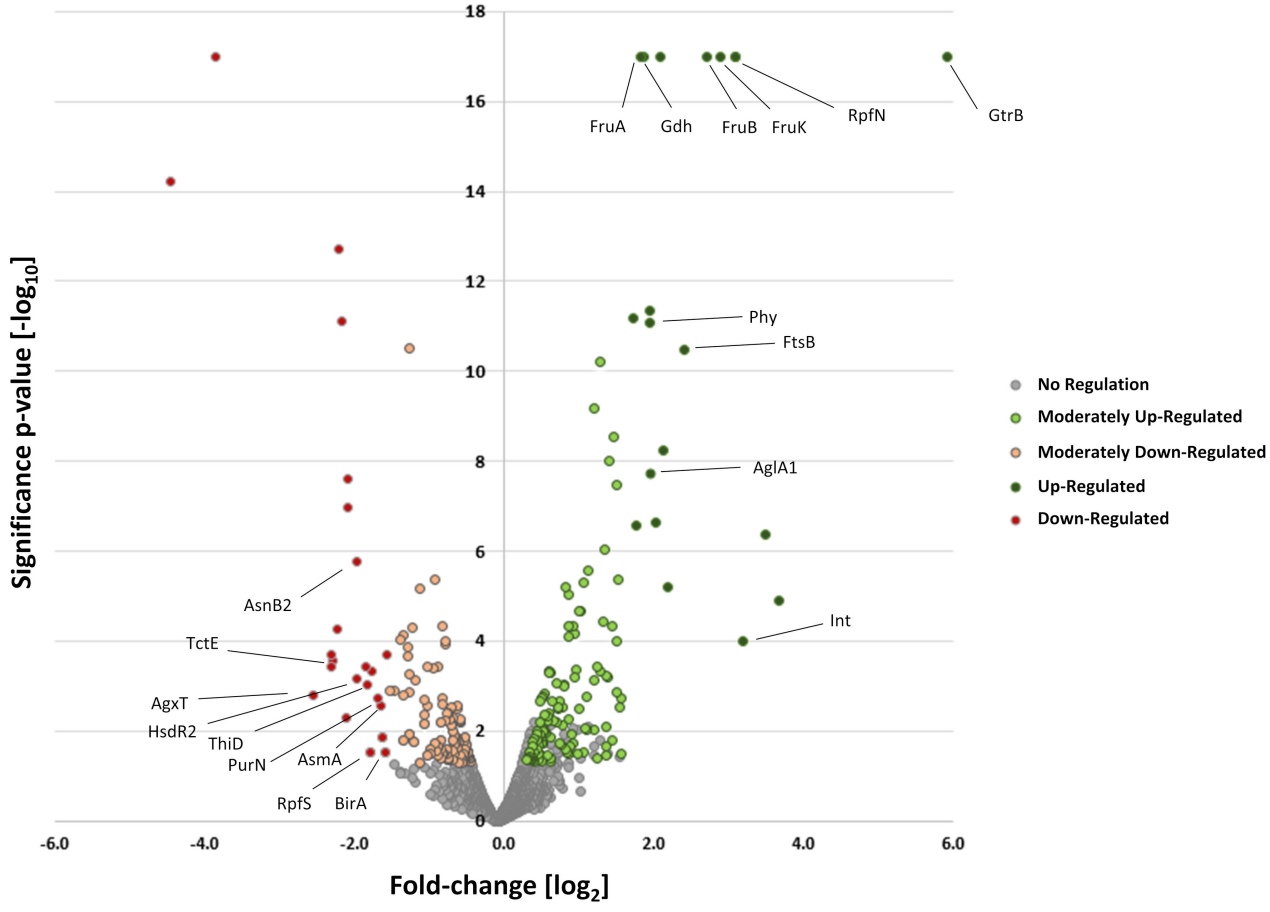


Fig. 4. Differential proteome analysis of the deletion mutant *Xcc* B100 *Δcrt1* compared to the wild-type strain.

Volcano plot obtained from proteome investigation of the strain *X. campestris* pv. campestris B100 *Δcrt1* compared to the wild-type strain *X. campestris* pv. campestris B100; cultivation was performed in the minimal XMD medium with 10 g/l glucose as a sole carbon source; Cells were harvested at an early stationary growth stage at an $oD_{600}$ nm of 1.8; shown are proteins with identified three unique peptides or more, and with peaks found for all replicates; green and red dots represent proteins with increased and decreased, respectively, abundance in the mutant strain *Xcc* B100 *Δcrt1*; cytosolic and membrane-bound proteins with expression unaffected by the deletion of *crt1* gene are represented by grey dots; annotated proteins with highest fold-change compared to the wild-type strain marked with their respective protein name.

*pilM* are located in close proximity on the genome, whereas *pilE* belongs to the operon situated afar from the *pil* gene cluster (Alkhateeb et al. 2016; Vorhölter et al. 2008). Among down-regulated genes, a target coding for sRNA denoted by its ORF *xccb100_rna193* was identified; it remains to be annotated and its biological functionality determined. However, small regulatory RNAs can modulate gene expression at the post-transcriptional level, thus complementing transcriptional regulators in their role in adapting bacteria to ever-changing environmental cues (Richards and Vanderpool, 2011; Storz et al. 2011). sRNA regulators were investigated in *Xanthomonas campestris* pv. *vesicatoria* (recently reclassified as *Xanthomonas euvesicatoria* pv. *euvesicatoria*), and further highly conserved sRNAs in *X. campestris* pv. *campestris* spp. were identified. Four novel regulatory units in *X. campestris* pv. *campestris* included sRNAs and are proposed to play an important post-transcriptional regulatory role in *X. campestris* pv. *campestris* spp. (Schmidtke et al. 2013). Interestingly, the small RNA *sX13*, also present in *X. campestris* pv. *campestris*, was shown to affect expression of the *hrp* regulon and type IV pilus biosynthesis, contributing to the regulation of bacterial virulence.

Differential transcriptional analysis revealed down-regulation of several targets that code for enzymes implicated in methionine utilization. However, methionine-related proteins do not act as virulence factors; they affect xanthan production. The "methionine effect" on xanthan biosynthesis has been investigated by various research groups. Supplementation of the culture media with 5 mM methionine resulted in a 40%

Table III
Effect of the regulator gene *crt1* deletion on transcriptome and proteome of *X. campestris* pv. campestris.

| Locus | Gene name | Function | COG | Fold-change | Transcript/ Protein abundance change | Studies in *Xanthomonas* |
|---|---|---|---|---|---|---|
| **Cell motility** | | | | | | |
| XCCB100_0954 | *pilM* | type IV pilus assembly protein | NU | 0.748 | T | Dugé de Bernonville et al, 2014 |
| XCCB100_0957 | *pilP* | Tfp pilus assembly protein | NU | 0.914 | T | Dugé de Bernonville et al, 2014 |
| XCCB100_1672 | *pilE* | Tfp pilus assembly protein | NU | 0.725 | T | Dugé de Bernonville et al, 2014 |
| **Carbohydrate transport and metabolism** | | | | | | |
| XCCB100_1697 | *aglA1* | alpha-glucosidase | G | 1.950 | P | Blanvillain et al, 2007; Fatima and Kumar, 2015; Eom et al. 2015; Ruan et al. 2014; Watt et al. 2009 |
| XCCB100_1799 | *rpfN* | carbohydrate-selective porin | G | 3.080 | P | Moreira et al. 2004 |
| XCCB100_1800 | *fruA* | PTS fructose porter | G | 1.820 | P | Moreira et al. 2004 |
| XCCB100_1801 | *fruK* | 1-phosphofructokinase | G | 2.890 | P | Li et al. 2019 |
| XCCB100_1802 | *fruB* | PTS fructose porter | G | -0.507 / 2.71 | T/P | Moreira et al. 2004 |
| **Signal transduction mechanisms and information processing** | | | | | | |
| XCCB100_0846 | *tctE* | two-component system sensor histidine kinase | T | -2.280 | P | Timilsina et al. 2020; Wang et al. 2016; Wang et al. 2017b |
| XCCB100_2607 | *rpfS* | DSF-sensing histidine kinase/ response regulator | T | -1.790 | P | An et al. 2014; O'Connell et al. 2013; Ryan et al. 2007 |
| **Amino acid transport and metabolism** | | | | | | |
| XCCB100_1297 | | homoserine O-acetyltransferase-like enzyme | | -1.204 | T | Pielken et al. 1987; Pielken et al. 1988; O'Connell et al. 2013 |
| XCCB100_1298 | *cgl* | cystathionine gamma-lyase | | -1.089 | T | Pielken et al. 1987; Pielken et al. 1988; O'Connell et al. 2013 |
| XCCB100_2099 | *hisH* | glutamine amidotransferase | | 0.766 | T | Li et al. 2019 |
| XCCB100_2866 | *asnB2* | asparagine synthase (glutamine-hydrolysing) | E | -1.950 | P | Qian et al. 2013 |
| **EPS biosynthesis** | | | | | | |
| AS_ XCCB100_1718** | | antisense transcript gumH | | 1.118 | T | Chan et al. 1999; Kiraly et al. 1997; Vojnov et al. 2001; Rigano et al. 2007; Alvarez et al. 2000; Yun et al. 2006 |
| XCCB100_1719 | *gumI* | mannosyltransferase | R | 0.726 | T | Chan et al. 1999, Kiraly et al. 1997; Vojnov et al. 2001; Rigano et al. 2007; Alvarez et al. 2000; Yun et al. 2006 |
| XCCB100_1720 | *gumJ* | xanthan repeating unit exporter | M | 0.833 | T | Chan et al. 1999, Kiraly et al. 1997; Vojnov et al. 2001; Rigano et al. 2007; Alvarez et al. 2000; Yun et al. 2006 |
| **Lipid transport and metabolism** | | | | | | |
| XCCB100_1788 | *phy* | putative exported phytase | I | 1.960 | P | Raboy 2003; Blüher et al, 2017; Chatterjee et al. 2003 |
| **Cell wall, membrane, envelope biogenesis** | | | | | | |
| XCCB100_1291 | *gtrB* | putative bactoprenol glucosyltransferase | | 5.92 | P | Newman et al. 2001; Vorhölter et al. 2001; Li et al. 2019 |
| **Other functions** | | | | | | |
| XCCB100_2558 | *ftsB* | septum formation initiator protein FtsB | D | 2.41 | P | Ferreira et al. 2017 |

Target genes, and cytosolic and membrane-bound proteins, involved or linked to the virulent life-style of *X. campestris* pv. campestris, with most significant abundance fold-change under deletion of crt1 gene as compared to the wild-type strain *X. campestris* pv. campestris B100; Abundance ratio represents the fold-change [log2] measured for replicates of deletion mutant relative to replicates of wild-type; Abundance ratio p-value has been calculated with significance background-based, nested ANOVA test, with n = 3; unique peptides describe how many peptides unique for a single target protein were employed for its identification.

decrease in xanthan biosynthesis (Pielken et al. 1987; Pielken et al. 1988). The findings could be reproduced in a more recent study of yet another LysR-family transcriptional regulator, CysB (Schulte et al. 2019). Although direct evidence could not be presented in our study so far, the fact of differentially expressed methionine-related targets strongly suggests links between the novel regulator and the "methionine effect", and further implies a putative link between methionine metabolism and virulence.

In bacteria, transcriptional regulators commonly cause a co-regulation of target genes, thus binding site motifs are usually conserved upstream of the transcription start sites of the respective genes. For the purpose of determining binding sites of novel regulator Crt1, sequences upstream of the transcription start sites (TSSs) of the considered target genes were analysed with the web-based tool MEME (Bailey et al. 2009). However, no such conserved motif could be found among the target genes identified in our study. We observed upregulation of transcripts within the gum cluster, which encodes proteins of the machinery necessary for xanthan production. Remarkably, among targets with the most significant fold-change as compared to the wild-type strain were those coding for factors essential for the virulent lifestyle of *X. campestris* pv. *campestris*, namely, T4P assembly proteins. Furthermore, the transcription of several methionine-related genes and sRNA with unknown functions was altered.

**Comparative investigation of cytosolic and membrane-proteome in *X. campestris* pv. *campestris* B100 *Δcrt1*.** To shed light on the more systemic effects of altered transcriptional regulation caused by the deletion of the crt1 gene, a comparative analysis of the cytosolic and membrane proteomes has been carried out. *X. campestris* pv. *campestris* was cultivated under identical conditions as those used for the whole-genome cDNA microarray experiments to correlate the results of both approaches. Mass spectrometry measurements of peptide samples were performed with a nanoLC coupled to a Q Exactive mass spectrometer (Thermo Fischer, USA). In total, 2871 proteins were identified representing 64% of all proteins encoded within *X. campestris* pv. *campestris* genome. The comparative investigation of the cytosolic and membrane proteomes was completed using a background-based, nested ANOVA test. This resulted in the identification of 63 proteins with fold-change ($\log_2$) of abundance compared to the wild-type strain of ≥ 1, and 58 proteins with fold-change of ≤ - 1, at a confidence level of at least 99% (Fig. 4). Identified proteins with the highest fold-change in abundance in the deletion mutant are presented in Table II, and the list of all proteins with statistically significant fold-change is presented in Supplementary Table V.

Among intracellular and membrane-bound proteins with enhanced abundance upon deletion of the *crt1* gene were RpfN, FruAB, and FruK, encoded by genes within a single operon. FruA and FruB form an active phosphotransferase system (PTS) fructose importer. 1-phosphofructokinase FruK transfers phosphate to the imported fructose moiety (Dills et al. 1980). One of the factors contributing to the successful *X. campestris* pv. *campestris* colonization of the host plant relies on the ability to efficiently use nutrients provided by the invaded host cell. Degradation of the plant cell wall produces a set of sugars, including fructose. Bacteria use PTS systems for the uptake of the degraded cell wall compounds (Moreira et al. 2004), as the FruAB PTS-importer mentioned above. The pathogenicity factor RpfN is a highly conserved regulator throughout the genus *Xanthomonas* and has been proposed as an outer-membrane porin or a glucose-sensitive porin.

In the deletion mutant *X. campestris* pv. *campestris* B100 *Δcrt1*, we measured remarkably elevated protein abundance of another protein involved in carbohydrate utilization, α-glucosidase AglA1, with a fold-change ($\log_2$) value of 1.87. As part of the sucrose and starch metabolism, it catalyses the hydrolysis of the terminal 1,4-linked αD-glucose residues from sucrose to form D-fructose. Significantly increased level of GtrB, a glucosyl transferase responsible for the transfer of sugar moieties onto the O-antigen component of the lipopolysaccharide was observed. The O-antigen polysaccharide side chain, together with the core oligosaccharide, forms an important surface-associated virulence factor, the lipopolysaccharide (LPS) (Newman et al. 2001; Vorhölter et al. 2001). It is involved in adhesion processes and protects bacteria from the environmental conditions (Braun et al. 2005; Desaki et al. 2006; Meyer et al. 2001).

We detected a decrease in the abundance of the two-component system sensor histidine kinase, TctE, in *X. campestris* pv. *campestris* B100 Δ*crt1*. TctE, together with the corresponding response regulator TctD, controlled the expression of *citH* gene in *Xanthomonas campestris* pv. *vesicatoria* (recently reclassified as *Xanthomonas euvesicatoria* pv. *euvesicatoria)* in a culture as well as *in planta* and affected bacterial growth on citrate (Tamir-Ariel et al. 2011). Two-component signal transduction systems function in bacteria as part of the

adaptation mechanism to ever-changing environmental stimuli (Hoch, 2000; Stock et al. 2000). Noteworthy is the significantly attenuated abundance of further histidine sensor kinase RpfS, which contains a C-terminal receiver (REC) domain, and an N-terminal Per/Arnt/Sim (PAS) domain with affinity to the diffusible signal factor (DSF), a key player of QS (An et al. 2014). DSF signalling is implicated in regulation of factors involved in pathogenicity (Ryan et al. 2011). More thoroughly investigated, DSF signal perception and transduction involve a two-component system, RpfC-RpfG. Transcriptional analysis of both RpfS and tandem RpfC/RpfG revealed a divergent subset of regulated target genes, with RpfS controlling the expression of genes involved in Type IV secretion and chemotaxis (An et al. 2013; An et al. 2014; O'Connell et al. 2013; Ryan et al. 2011). Mutations in RpfS decreased virulence of *Xanthomonas* solely upon spraying the bacteria onto leaf tissue of the host plant but had no effect on infection symptoms after introducing the bacteria directly into the leaf vascular system. The former requires motility for *X. campestris* pv. *campestris* to move towards the hydathodes, hence showing involvement of RpfS in DSF-dependent regulation of chemotaxis and motility (An et al. 2014). Another protein regulated by the DSF, which demonstrated significantly altered abundance in the mutant *X. campestris* pv. *campestris* B100 *Δcrt1* was asparagine synthase AsnB2. The measured fold-change ($log_2$) compared to the wild-type strain *X. campestris* pv. *campestris* B100 was -1.95. In *Xanthomonas oryzae*, AsnB was shown to be regulated by both DSF and the global regulator Clp, and AsnB was found to be involved not only in aspartate metabolism but also in resistance to oxidative stress, virulence, and the regulation of several virulence-related genes (Qian et al. 2013).

Remarkably, among proteins with the highest fold-change increase upon deletion of the *crt1* gene, was putative phytase Phy (ORF *xccb100_1788*). Phytases are capable of dephosphorylating myo-inositol-hexakisphosphate ($InsP_6$, phytate), which is the major phosphate storage in plant seeds, and is involved in defense mechanisms of the host plant against pathogens (Raboy, et al. 2003). In *Xanthomonas*, the Type III effector XopH was shown to have phytase activity that interferes with plant hormone pathways (Blüher et al. 2017). Chatterjee et al. (2003) suggest that the phytase PhyA contributes to scavenging more phosphate from plant tissue, thus improving the nutritional status of *Xanthomonas*.

*X. campestris* pv. *campestris* B100 *Δcrt1* mutant demonstrated a significant increase in the abundance of the septum formation initiator protein FtsB. FtsB, together with FtsL and FtsQ, form a macromolecular complex that facilitates coordinated invagination of the plasma membrane and peptidoglycan wall (Villanelo et al. 2011). In a recent study, Ferreira et al. (2017) conducted a screening of a mutant library of *Xanthomonas citri* to identify novel genes involved in adaptation and virulence that had not previously been implicated in the virulence of *Xanthomonas*. Mutants with a disrupted *ftsB* gene were unable to induce hyperplasia and showed reduced necrosis in the infected host plant.

Among identified targets with increased abundance in the deletion mutant compared to the wild-type strain was glutamate dehydrogenase Gdh (ORF XCCB100_1807), which is involved in glutamate metabolism. L-glutamate is fundamental for growth in *Xanthomonas* and plays a central role in nitrogen metabolism, an important factor in xanthan production (Rojas et al. 2013; Soares et al. 2010).

Noteworthy as well is the significantly altered expression of two putative transcriptional regulators. Deletion of *crt1* resulted in increased abundance of a yet non-characterized Crp-family transcriptional regulator encoded by the gene *xccb100_2092*. Significantly decreased levels were observed for the non-annotated LysR family transcriptional regulator (XCCB100_3906). Interestingly, the latter (XCCB100_3906) contains a conserved PucR-like DNA-binding domain and a substrate-binding domain of CysB type that depends on intermediates of the sulphur metabolism (Beier et al. 2002; Tyrrell et al. 1997). Nevertheless, the function of regulators with the most significant fold-change in *X. campestris* pv. *campestris* B100 Δ*crt1* can only be speculated on at the present state of knowledge.

Considering the cytosolic and membrane proteins with the most significant fold-change of abundance, we inspected the respective transcriptional differences between the deletion mutant and the wild-type strain. We observed that genes coding for the above-mentioned proteins were not among the targets with the highest transcript fold changes.

**Crt1 regulation of factors involved in the pathogenicity of *X. campestris* pv. *campestris*.** This investigation revealed altered expression of various factors involved in the virulent lifestyle of *X. campestris* pv. *campestris* or linked to the pathogenicity (Table III). In the study, transcriptional upregulation of the motility-related genes *pilP*, *pilM*, and *pilE* was demonstrat-

ed. This observation indicates that Crt1 officiates as a repressor of pilus assembly genes. Dugé de Bernonville (et al. 2014) conducted cDNA microarray-based transcriptome analysis of *X. campestris* pv. *campestris* cultivated in xylem sap. The study showed transcriptional reprogramming of genes encoding TonB-dependent transporters and upregulation of twitching motility-related genes, including type IV pilus assembly protein-encoding genes. Upon colonization of the *Brassicaceae*, phytopathogens like *X. campestris spp.* initially penetrate xylem elements of the vascular systems of the host plant or intercellular spaces of the mesophyll parenchyma (Ryan et al. 2011). Hence, identified target genes with altered transcription upon *crt1* deletion are necessary for *X. campestris* pv. *campestris* to adapt to the novel environment and host-derived metabolites and defense mechanisms.

Most bacteria utilize two-component signal transduction systems as part of their adaptation to ever-changing environmental stimuli (Hoch, 2000; Stock et al. 2000). Extraordinarily, decreased abundance of two separate two-component system sensor histidine kinases, namely TctE and RpfS, was observed in this study. Histidine kinases (HK) of *X. campestris* pv. *campestris* are usually membrane-bound and paired with a cytosolic response regulator (RR) that conducts downstream regulation (Bourret and Silversmith 2010). Within the genome of *X. campestris* pv. *campestris* there are 53 genes coding for HKs, classified in three groups according to their membrane topology (Qian et al. 2008a; Qian et al. 2008b). So far, only several HKs have been investigated in *X. campestris* pv. *campestris*, among others RpfC, VgrS (ColS), PcrK, RavS or HpaS. All of the aforementioned have been implicated in the modulation of virulence, thus facilitating coordinated bacterial lifestyle transition between free swimming and virulence (Büttner and Bonas 2010; Cheng et al. 2019; Qian et al. 2008a; Tang et al. 1991; Timilsina et al. 2020; Wang et al. 2016; Wang et al. 2017a). The HK RpfC coupled with RR RpfG are encoded within the ***r**egulation of **p**athogenicity **f**actors* (*rpf*) gene cluster (Crossman and Dow 2004; Dow et al. 2003). Upon DSF recognition, RpfG hydrolyses the second messenger cyclic di-GMP, thereby averting the repression of another important QS regulator, namely Clp. Both cyclic-di-GMP and Clp contribute to the pathogenicity of *X. campestris* pv. *campestris*, as they regulate various virulence factors (Büttner and Bonas, 2010; McCarthy et al. 2008; Ryan et al. 2007; Simm et al. 2004; Tischler and Camilli 2004). In this study, the sensor histidine kinase RpfS was found to be upregulated upon deletion of the regulator gene *crt1.* RpfS was identified to be involved in DSF-dependent signalling, alongside RpfC-RpfG, with two-component systems controlling two separate subsets of target genes. RpfS regulated the expression of genes involved in T4 secretion and chemotaxis (An et al. 2013; An et al. 2014; O'Connell et al. 2013; Ryan et al. 2011). Furthermore, mutations in the rpfS gene resulted in decreased virulence of *Xanthomonas*, as intact motility was required to enable entry into the hydathodes. This leads to the conclusion that Crt1 conducts more sophisticated, complex regulation, suggesting that the novel regulator might be responsible for fine-tuning within the regulatory network of virulence factors. The biological importance of TctE was shown in a study on *Xanthomonas campestris* pv. *vesicatoria* (recently reclassified as *Xanthomonas euvesicatoria* pv. *euvesicatoria*). The two-component system TctE-TctD controlled the expression of the *citH* gene in a culture as well as *in planta* and affected bacterial growth on citrate (Tamir-Ariel et al. 2011).

*X. campestris* pv. *campestris* employs the type III secretion system (T3SS), encoded by genes within the hrp (hypersensitive response and pathogenicity) cluster, to translocate type III effector proteins (T3Es) into the host plant cell cytoplasm. A distinct family of T3Es, known as **t**ranscription **a**ctivation-**l**ike **e**ffectors (TALEs) modulate the transcription of host immunity-related genes, as well as genes encoding for sugar biosynthesis and exporter systems (SWEET) of the plant, as a strategy to acquire nutrients from the host tissue (Boch and Bonas 2010; Cohn et al. 2014; Cox et al. 2017; Fatima and Kumar 2015; da Silva et al. 2002; Timilsina et al. 2020). TALEs of other *Xanthomona*s species were demonstrated to induce the expression of SWEET11 and SWEET13 transporter systems in rice, which promote the efflux of glucose and sucrose, respectively (Chen et al. 2010; Eom et al. 2015; Zhou et al. 2015). Sucrose is regarded as a major transport carbohydrate *in planta,* essential for the growth of *Xanthomonas* upon colonization (Blanvillain et al. 2007; Eom et al. 2015; Fatima and Kumar 2015; Ruan 2014; Watt et al. 2009).

Considering the fact that Crt1 has been identified as a sucrose-related transcriptional regulator (Leßmeier et al. 2016), it is strongly suggested that the Crt1-directed repression is a part of the aforementioned plant-affiliated transcriptional reprogramming.

The limited overlap observed between transcriptomic and proteomic datasets is likely due to post-tran-

scriptional and post-translational regulation, including differences in mRNA stability, translation efficiency, and protein turnover. Additionally, technical factors such as the dynamic range of protein detection and sampling may contribute to the discrepancies observed at both levels of investigation. Despite these limitations, the proteomic data provide valuable insights into the functional consequences of transcriptional regulator Crt1 deletion. We detected significantly increased protein abundance of α-glucosidase AglA1 in the deletion mutant *X. campestris* pv. *campestris* B100 *Δcrt1*. AglA1 hydrolyses sucrose to D-fructose as part of sucrose and starch metabolism, hence it is involved in the utilization of plant-based carbohydrates. Furthermore, we measured elevated levels of the RpfN, FruAB, and FruK proteins, encoded by a single operon and involved in fructose import and intracellular metabolism. Moreover, we detected elevated levels of putative phytase, annotated as Phy (XCCB100_1788), in the deletion mutant *X. campestris* pv. *campestris* B100 *Δcrt1*. The enzyme can dephosphorylate a major phosphate storage in plant seeds, phytate, and has been speculated to be involved in scavenging plant-based phosphate (Chatterjee et al. 2003; Raboy et al. 2003). Another study revealed that essential T3E XopH exerts its role through phytase activity and interferes with plant hormone pathways (Blüher et al. 2017). This reinforces the findings of this study that regulator Crt1 is involved in the re-programming of the *X. campestris* pv. *campestris* lifestyle to ensure a more efficient reclaim of nutrients from the invaded host plant tissue.

*X. campestris* pv. *campestris* produces the exopolysaccharide (EPS) xanthan, which, due to its physicochemical features, contributes to protection against environmental stresses, such as desiccation or damage by reactive oxygen species (ROS) (Kiraly et al. 1997; Vojnov et al. 2001). EPS biosynthesis in *Xanthomonas* was correlated with the attachment to host plant tissue and biofilm formation (Rigano et al. 2007). EPS is implied to prevent host plants from recognizing *X. campestris* pv. *campestris* and thus facilitates the successful colonization of the plant tissue (Alvarez, et al. 2000). It was also shown that xanthan causes wilting of host plants by blocking water flow in xylem vessels (Chan and Goodwin, 1999). EPS has also been implicated in suppressing callose deposition in the plant cell wall, a basal plant defense response, by binding extracellular calcium ions (Yun et al. 2006).

In this study, the generation of EPS xanthan was almost 40% higher in the deletion mutant than in the wild-type strain *X. campestris* pv. *campestris* B100. Moreover, a significant upregulation of the *antisense gumH* transcript abundance, as well as of the downstream genes, was observed in the mutant strain. The further downstream of *gumH*, the less significant was the fold-change of transcript levels between the deletion mutant and the wildtype strain. Proteins required for xanthan production and the export machinery are encoded by twelve genes contained within the *gum* cluster (Katzen et al. 1996; Katzen et al. 1998; Vojnov et al. 2001; Vorhölter et al. 2008). The expression of the *gum* operon was proposed to be directed by two promoter regions – one located upstream of *gumB*, and the second weak promoter located upstream of *gumK* (Katzen et al. 1996). Investigation of the TSSs of *X. campestris* pv. *campestris* B100 led to the identification of additional transcriptional initiation sites within the operon – additional active primary TSS were identified upstream of *gumD* and *gumH* (Alkhateeb et al. 2016). Furthermore, the study led to the detection of five antisense TSSs on the opposite strand of *gumB*, *gumD*, *gumE*, *gumH*, and *gumK*. We observed only moderate up-regulation of six of the twelve *gum* genes - *gumE, gumI, gumJ, gumK, gumL,* and *gumM* in the deletion mutant strain, with the highest fold-change identified within the transcript of the antisense TSS of *gumH* (Table I and Supplementary Table IV).

Among the surface-associated virulence factors are lipopolysaccharides (LPS), consisting of membrane-anchored lipid A, a core oligosaccharide, and O-antigen polysaccharide side chains (Newman et al. 2001; Vorhölter et al. 2001). The O-antigen polysaccharide is involved in adhesion processes and protection from adverse environmental conditions and thus favors the virulence of *X. campestris* pv. *campestris*. A significant increase in the abundance of GtrB, a glucosyl transferase involved in the synthesis of O-antigen was detected in the Crt1 mutant. The ties between GtrB and Quorum Sensing were demonstrated by *in planta* DSF/Rpf-mediated upregulation of gene expression of *gtrb* gene in *Xca* during early stages of host infection (Li et al.2019). As described previously, DSF and RpfC-RpfG component systems are involved in QS, regulating the expression of diverse traits in *Xanthomonas* spp., including those responsible for the virulent behavior of bacteria (Li et al, 2019). The schematic network of factors regulated by Crt1 and their interactions with virulence-secretion systems is depicted in Fig. 5.

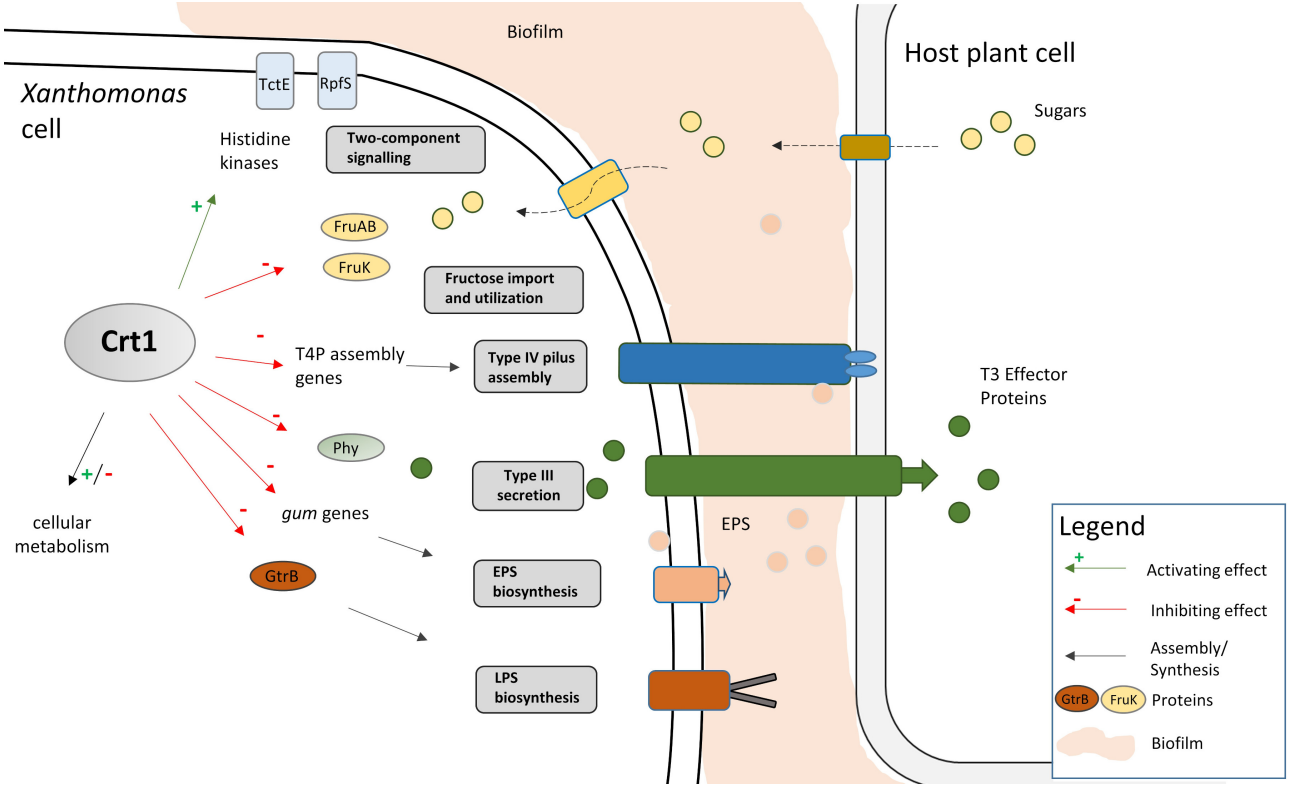


Fig. 5. Regulatory network of the carbohydrate related transcription factor Crt1 in *Xanthomonas campestris* pv. campestris.

Depicted is the schematic view of the regulatory network that is influenced by the novel regulator Crt1, as well as different virulence factors in *X. campestris* pv. campestris. Activating effect of Crt1 is denoted by green arrows with "+"; inhibiting effect is denoted by red arrows with "–". Virulence of *X. campestris* pv. campestris depends on T3S system, adhesion provided by T4 pilus, EPS, and LPS. T3S system translocates T3 effector proteins into the host plant cell, where they can modulate host gene expression. T3 effectors may also activate plant defense response cues. The adaptation of *X. campestris* pv. campestris lifestyle during infection includes regulation of import and utilization of plant-derived nutrients. Crt1 regulates virulence factors involved in T4P assembly, EPS and LPS biosynthesis, signaling transduction and utilization of plant-related nutrients. Furthermore, novel regulator affects enzymes implicated in methionine metabolism.

## Conclusion

In summary, with this work, we introduced the transcriptional regulator Crt1 and demonstrated in a *multi-omics* approach that it regulates a variety of virulence factors, including those involved in T4P assembly, EPS and LPS biosynthesis, signalling, and utilization of plant-related nutrients. The findings have been confirmed by the pathogenicity assay conducted on *Br. oleracea*. Infection of the host plant tissue caused by the deletion mutant *X. campestris* pv. *campestris* B100 Δ*crt1* was significantly more severe than by the wild-type strain. Hence, the transcriptional regulator Crt1 we introduce and characterize in this study is involved in the modulation of virulence factors and influences the pathogenic lifestyle of *X. campestris* pv. *campestris*. However, under the deletion of the *crt1* gene, merely 11 genes were significantly altered in their transcription (fold-change[log2] |M-value| of ≥ 1), and 118 proteins were differentially expressed (|abundance fold-change ($\log_2$) | ≥1). This finding underscores that Crt1 does not act as a global regulator yet controls the expression of numerous targets. Therefore, it is predicted to be a mid-tier regulator involved in re-programming during the early stage of bacterial infection.

**Acknowledgments**
The authors would also like to thank our cooperation partners from Jungbunzlauer Austria AG for the financial support of this project.

**Conflict of interest**
The authors do not report any financial or personal connections with other persons or organizations, which might negatively affect the contents of this publication and/or claim authorship rights to this publication.

## Literature

**Alkhateeb RS**, **Vorhölter F-J**, **Rückert C**, **Mentz A**, **Wibberg D**, **Hublik G**, **Niehaus K**, **Pühler A**. 2016. Genome wide transcription start sites analysis of *Xanthomonas campestris* pv. *campestris* B100 with insights into the gum gene cluster directing the biosynthesis of the exopolysaccharide xanthan. *J Biotechnol*. 225:18–28. https://doi.

org/10.1016/j.jbiotec.2016.03.020

**Alkhateeb RS**, **Vorhölter F-J**, **Steffens T**, **Rückert C**, **Ortseifen V**, **Hublik G**, **Niehaus K**, **Pühler A**. 2018. Comparative transcription profiling of two fermentation cultures of *Xanthomonas campestris* pv. *campestris* B100 sampled in the growth and in the stationary phase. *Appl Microbiol Biotechnol*. 102(15):6613–6625. https://doi.org/10.1007/s00253-018-9106-2

**Alvarez AM**. 2000. Black rot of crucifers. In: Slusarenko AJ, Fraser RSS, Van Loon LC, editors. *Mechanisms of resistance to plant diseases*. Dordrecht: Springer. p. 21–52. https://doi.org/10.1007/978-94-011-3937-3_2

**An S**, **Allan JH**, **McCarthy Y**, **Febrer M**, **Dow JM**, **Ryan RP**. 2014. The PAS domain-containing histidine kinase RpfS is a second sensor for the diffusible signal factor of *Xanthomonas campestris*. *Mol Microbiol*. 92(3):586–597. https://doi.org/10.1111/mmi.12577

**An S**, **Febrer M**, **McCarthy Y**, **Tang D**, **Clissold L**, **Kaithakottil G**, **Swarbreck D**, **Tang J**, **Rogers J**, **Dow JM**, **et al.** 2013. High-resolution transcriptional analysis of the regulatory influence of cell-to-cell signalling reveals novel genes that contribute to *Xanthomonas* phytopathogenesis. *Mol Microbiol*. 88(6):1058–1069. https://doi.org/10.1111/mmi.12229

**Bailey TL**, **Boden M**, **Buske FA**, **Frith M**, **Grant CE**, **Clementi L**, **Ren J**, **Li WW**, **Noble WS**. 2009. MEME SUITE: tools for motif discovery and searching. *Nucleic Acids Res*. 37(Web Server issue):W202–W208. https://doi.org/10.1093/nar/gkp335

**Bansal K**, **Kumar S**, **Singh A**, **Chaudhary A**, **Patil PB**. 2023. Redefining the taxonomic boundaries of the genus *Xanthomonas*. *Taxonomy*. 3(4):452–465. https://doi.org/10.3390/taxonomy3040026

**Beier L**, **Nygaard P**, **Jarmer H**, **Saxild HH**. 2002. Transcription analysis of the *Bacillus subtilis* PucR regulon and identification of a cis-acting sequence required for PucR-regulated expression of genes involved in purine catabolism. *J Bacteriol*. 184(12):3232–3241. https://doi.org/10.1128/JB.184.12.3232-3241.2002

**Beringer JE**. 1974. R factor transfer in *Rhizobium leguminosarum*. *J Gen Microbiol*. 84(1):188–198. https://doi.org/10.1099/00221287-84-1-188

**Bertoni M**, **Kiefer F**, **Biasini M**, **Bordoli L**, **Schwede T**. 2017. Modeling protein quaternary structure of homo- and hetero-oligomers beyond binary interactions by homology. *Sci Rep*. 7(1):10480. https://doi.org/10.1038/s41598-017-09654-8

**Blanvillain S**, **Meyer D**, **Boulanger A**, **Lautier M**, **Guynet C**, **Denancé N**, **Vasse J**, **Lauber E**, **Arlat M**. 2007. Plant carbohydrate scavenging through TonB-dependent receptors: a feature shared by phytopathogenic and aquatic bacteria. *PLoS One*. 2(2):e224. https://doi.org/10.1371/journal.pone.0000224

**Blüher D**, **Laha D**, **Thieme S**, **Hofer A**, **Eschen-Lippold L**, **Masch A**, **Balcke G**, **Pavlovic I**, **Nagel O**, **Schonsky A**, **et al.** 2017. A 1-phytase type III effector interferes with plant hormone signaling. *Nat Commun*. 8(1):2159. https://doi.org/10.1038/s41467-017-02195-8

**Boch J**, **Bonas U**. 2010. *Xanthomonas* AvrBs3 family-type III effectors: discovery and function. *Annu Rev Phytopathol*. 48:419–436. https://doi.org/10.1146/annurev-phyto-080508-081936

**Bonas U**, **Van den Ackerveken G**, **Büttner D**, **Hahn K**, **Marois E**, **Nennstiel D**, **Noel L**, **Rossier O**, **Szurek B**. 2000. How the bacterial plant pathogen *Xanthomonas campestris* pv. *vesicatoria* conquers the host. *Mol Plant Pathol*. 1(1):73–76. https://doi.org/10.1046/j.1364-3703.2000.00010.x

**Bourret RB**, **Silversmith RE**. 2010. Two-component signal transduction. *Curr Opin Microbiol*. 13(2):113–115. https://doi.org/10.1016/j.mib.2010.02.003

**Bradbury JF**. 1986. *Guide to plant pathogenic bacteria*. Farnham Royal (UK): CAB International.

**Braun SG**, **Meyer A**, **Holst O**, **Pühler A**, **Niehaus K**. 2005. Characterization of the *Xanthomonas campestris* pv. *campestris* lipopolysaccharide substructures essential for elicitation of an oxidative burst in tobacco cells. *Mol Plant Microbe Interact*. 18(7):674–681. https://doi.org/10.1094/MPMI-18-0674

**Burkholder WH**. 1957. Genus II. *Xanthomonas*. In: **Breed RS**, **Murray EGD**, **Smith NR**, editors. *Bergey's manual of determinative bacteriology*. 7th ed. Baltimore (MD): Williams & Wilkins. p. 152–183.

**Büttner D**, **Bonas U**. 2010. Regulation and secretion of *Xanthomonas* virulence factors. *FEMS Microbiol Rev*. 34(2):107–133. https://doi.org/10.1111/j.1574-6976.2009.00192.x

**Chan JWYF**, **Goodwin PH**. 1999. The molecular genetics of virulence of *Xanthomonas campestris*. *Biotechnol Adv*. 17(6):489–508. https://doi.org/10.1016/S0734-9750(99)00025-7

**Chatterjee S**, **Sankaranarayanan R**, **Sonti RV**. 2003. PhyA, a secreted protein of *Xanthomonas oryzae* pv. *oryzae*, is required for optimum virulence and growth on phytic acid as a sole phosphate source. *Mol Plant Microbe Interact*. 16(11):973–982. https://doi.org/10.1094/MPMI.2003.16.11.973

**Chen L-Q**, **Hou B-H**, **Lalonde S**, **Takanaga H**, **Hartung ML**, **Qu X-Q**, **Guo W-J**, **Kim J-G**, **Underwood W**, **Chaudhuri B**, **et al.** 2010. Sugar transporters for intercellular exchange and nutrition of pathogens. *Nature*. 468(7323):527–532. https://doi.org/10.1038/nature09606

**Cheng S-T**, **Wang F-F**, **Qian W**. 2019. Cyclic-di-GMP binds to histidine kinase RavS to control RavS–RavR phosphotransfer and regulates the bacterial lifestyle transition between virulence and swimming. *PLoS Pathog*. 15(8):e1007952. https://doi.org/10.1371/journal.ppat.1007952

**Cohn M**, **Bart RS**, **Shybut M**, **Dahlbeck D**, **Gomez M**, **Morbitzer R**, **Hou B-H**, **Frommer WB**, **Lahaye T**, **Staskawicz BJ**. 2014. *Xanthomonas axonopodis* virulence is promoted by a transcription activator-like effector–mediated induction of a SWEET sugar transporter in cassava. *Mol Plant Microbe Interact*. 27(11):1186–1198. https://doi.org/10.1094/MPMI-06-14-0161-R

**Cox KL**, **Meng F**, **Wilkins KE**, **Li F**, **Wang P**, **Booher NJ**, **Carpenter SCD**, **Chen L-Q**, **Zheng H**, **Gao X**, **et al.** 2017. TAL effector driven induction of a SWEET gene confers susceptibility to bacterial blight of cotton. *Nat Commun*. 8(1):15588. https://doi.org/10.1038/ncomms15588

**Crossman L**, **Dow JM**. 2004. Biofilm formation and dispersal in *Xanthomonas campestris*. *Microbes Infect*. 6(6):623–629. https://doi.org/10.1016/j.micinf.2004.01.013

**Da Silva ACR**, **Ferro JA**, **Reinach FC**, **Farah CS**, **Furlan LR**, **Quaggio RB**, **Monteiro-Vitorello CB**, **Van Sluys MA**, **Almeida NF**, **Alves LMC**, **et al.** 2002. Comparison of the genomes of two *Xanthomonas* pathogens with differing host specificities. *Nature*. 417(6887):459–463. https://doi.org/10.1038/417459a

**Desaki Y**, **Miya A**, **Venkatesh B**, **Tsuyumu S**, **Yamane H**, **Kaku H**, **Minami E**, **Shibuya N**. 2006. Bacterial lipopolysaccharides induce defense responses associated with programmed cell death in rice cells. *Plant Cell Physiol*. 47(11):1530–1540. https://doi.org/10.1093/pcp/pcl019

**Déziel E**, **Gopalan S**, **Tampakaki AP**, **Lépine F**, **Padfield KE**, **Saucier M**, **Xiao G**, **Rahme LG**. 2005. The contribution of MvfR to *Pseudomonas aeruginosa* pathogenesis and quorum sensing circuitry regulation. *Mol Microbiol*. 55(4):998–1014. https://doi.org/10.1111/j.1365-2958.2004.04448.x

**Dills SS**, **Apperson A**, **Schmidt MR**, **Saier MH**. 1980. Carbohydrate transport in bacteria. *Microbiol Rev*. 44(3):385–418. https://doi.org/10.1128/mr.44.3.385-418.1980

**Dondrup M**, **Albaum SP**, **Griebel T**, **Henckel K**, **Jünemann S**, **Kahlke T**, **Kleindt CK**, **Küster H**, **Linke B**, **Mertens D**, **et al.** 2009. EMMA 2 – a MAGE-compliant system for the collaborative analysis and integration of microarray data. *BMC Bioinformatics*.

10(1):50. https://doi.org/10.1186/1471-2105-10-50

**Dow JM**, **Crossman L**, **Findlay K**, **He Y-Q**, **Feng J-X**, **Tang J-L**. 2003. Biofilm dispersal in *Xanthomonas campestris* is controlled by cell–cell signaling and is required for full virulence to plants. *Proc Natl Acad Sci U S A*. 100(19):10995–11000. https://doi.org/10.1073/pnas.1833360100

**Droste J**, **Ortseifen V**, **Schaffert L**, **Persicke M**, **Schneiker-Bekel S**, **Pühler A**, **Kalinowski J**. 2020. The expression of the acarbose biosynthesis gene cluster in *Actinoplanes* sp. SE50/110 is dependent on the growth phase. *BMC Genomics*. 21(1):818. https://doi.org/10.1186/s12864-020-07194-6

**Dugé de Bernonville T**, **Noël LD**, **SanCristobal M**, **Danoun S**, **Becker A**, **Soreau P**, **Arlat M**, **Lauber E**. 2014. Transcriptional reprogramming and phenotypical changes associated with growth of *Xanthomonas campestris* pv. *campestris* in cabbage xylem sap. *FEMS Microbiol Ecol*. 89(3):527–541. https://doi.org/10.1111/1574-6941.12345

**Eom J-S**, **Chen L-Q**, **Sosso D**, **Julius BT**, **Lin I**, **Qu X-Q**, **Braun DM**, **Frommer WB**. 2015. SWEETs, transporters for intracellular and intercellular sugar translocation. *Curr Opin Plant Biol*. 25:53–62. https://doi.org/10.1016/j.pbi.2015.04.005

**Fatima U**, **Senthil-Kumar M**. 2015. Plant and pathogen nutrient acquisition strategies. *Front Plant Sci*. 6:750. https://doi.org/10.3389/fpls.2015.00750

**Ferreira CB**, **Moreira LM**, **Brigati JB**, **Lima LL**, **Ferro JA**, **Ferro MIT**, **Oliveira JCFD**. 2017. Identification of new genes related to virulence of *Xanthomonas axonopodis* pv. *citri* during citrus host interactions. *Adv Microbiol*. 7(1):22–46. https://doi.org/10.4236/aim.2017.71003

**Gibson DG**, **Young L**, **Chuang R-Y**, **Venter JC**, **Hutchison CA**, **Smith HO**. 2009. Enzymatic assembly of DNA molecules up to several hundred kilobases. *Nat Methods*. 6(5):343–345. https://doi.org/10.1038/nmeth.1318

**Green MR**, **Sambrook J**. 2012. *Molecular cloning: a laboratory manual*. New York (NY): Cold Spring Harbor Laboratory Press.

**Guex N**, **Peitsch MC**, **Schwede T**. 2009. Automated comparative protein structure modeling with SWISS-MODEL and Swiss-PdbViewer: a historical perspective. *Electrophoresis*. 30(S1):S162–S173. https://doi.org/10.1002/elps.200900140

**Hartmann T**, **Zhang B**, **Baronian G**, **Schulthess B**, **Homerova D**, **Grubmüller S**, **Kutzner E**, **Gaupp R**, **Bertram R**, **Powers R**, **et al.** 2013. Catabolite control protein E (CcpE) is a LysR-type transcriptional regulator of tricarboxylic acid cycle activity in *Staphylococcus aureus*. *J Biol Chem*. 288(50):36116–36128. https://doi.org/10.1074/jbc.M113.516302

**He Y-W**, **Zhang L-H**. 2008. Quorum sensing and virulence regulation in *Xanthomonas campestris*. *FEMS Microbiol Rev*. 32(5):842–857. https://doi.org/10.1111/j.1574-6976.2008.00120.x

**Heroven AK**, **Dersch P**. 2006. RovM, a novel LysR-type regulator of the virulence activator gene *rovA*, controls cell invasion, virulence and motility of *Yersinia pseudotuberculosis*. *Mol Microbiol*. 62(5):1469–1483. https://doi.org/10.1111/j.1365-2958.2006.05458.x

**Hilker R**, **Stadermann KB**, **Schwengers O**, **Anisiforov E**, **Jaenicke S**, **Weisshaar B**, **Zimmermann T**, **Goesmann A**. 2016. ReadXplorer 2—detailed read mapping analysis and visualization from one single source. *Bioinformatics*. 32(24):3702–3708. https://doi.org/10.1093/bioinformatics/btw541

**Hoch JA**. 2000. Two-component and phosphorelay signal transduction. *Curr Opin Microbiol*. 3(2):165–170. https://doi.org/10.1016/S1369-5274(00)00070-9

**Jun S-R**, **Sims GE**, **Wu GA**, **Kim S-H**. 2010. Whole-proteome phylogeny of prokaryotes by feature frequency profiles: an alignment-free method with optimal feature resolution. *Proc Natl Acad Sci U S A*. 107(1):133–138. https://doi.org/10.1073/pnas.0913033107

**Katzen F**, **Becker A**, **Zorreguieta A**, **Pühler A**, **Ielpi L**. 1996. Promoter analysis of the *Xanthomonas campestris* pv. *campestris* gum operon directing biosynthesis of the xanthan polysaccharide. *J Bacteriol*. 178(14):4313–4318. https://doi.org/10.1128/jb.178.14.4313-4318.1996

**Katzen F**, **Ferreiro DU**, **Oddo CG**, **Ielmini MV**, **Becker A**, **Pühler A**, **Ielpi L**. 1998. *Xanthomonas campestris* pv. *campestris* gum mutants: effects on xanthan biosynthesis and plant virulence. *J Bacteriol*. 180(7):1607–1617. https://doi.org/10.1128/JB.180.7.1607-1617.1998

**Király Z**, **El-Zahaby HM**, **Klement Z**. 1997. Role of extracellular polysaccharide (EPS) slime of plant pathogenic bacteria in protecting cells to reactive oxygen species. *J Phytopathol*. 145(2–3):59–68. https://doi.org/10.1111/j.1439-0434.1997.tb00365.x

**Leßmeier L**, **Alkhateeb RS**, **Schulte F**, **Steffens T**, **Loka TP**, **Pühler A**, **Niehaus K**, **Vorhölter F-J**. 2016. Applying DNA affinity chromatography to specifically screen for sucrose-related DNA-binding transcriptional regulators of *Xanthomonas campestris*. *J Biotechnol*. 232:89–98. https://doi.org/10.1016/j.jbiotec.2016.04.007

**Li L**, **Li J**, **Zhang Y**, **Wang N**. 2019. Diffusible signal factor (DSF)-mediated quorum sensing modulates expression of diverse traits in *Xanthomonas citri* and responses of citrus plants to promote disease. *BMC Genomics*. 20(1):55. https://doi.org/10.1186/s12864-018-5384-4

**Maddocks SE**, **Oyston PCF**. 2008. Structure and function of the LysR-type transcriptional regulator (LTTR) family proteins. *Microbiology*. 154(12):3609–3623. https://doi.org/10.1099/mic.0.2008/022772-0

**McCarthy Y**, **Ryan RP**, **O'Donovan K**, **He Y**, **Jiang B**, **Feng J**, **Tang J**, **Dow JM**. 2008. The role of PilZ domain proteins in the virulence of *Xanthomonas campestris* pv. *campestris*. *Mol Plant Pathol*. 9(6):819–824. https://doi.org/10.1111/j.1364-3703.2008.00495.x

**Meyer A**, **Pühler A**, **Niehaus K**. 2001. The lipopolysaccharides of the phytopathogen *Xanthomonas campestris* pv. *campestris* induce an oxidative burst reaction in cell cultures of *Nicotiana tabacum*. *Planta*. 213(2):214–222. https://doi.org/10.1007/s004250000493

**Minezaki Y**, **Homma K**, **Nishikawa K**. 2006. Genome-wide survey of transcription factors in prokaryotes reveals many bacteria-specific families not found in archaea. *DNA Res*. 12(5):269–280. https://doi.org/10.1093/dnares/dsi016

**Moreira LM**, **De Souza RF**, **Almeida NF Jr**, **Setubal JC**, **Oliveira JCF**, **Furlan LR**, **Ferro JA**, **Da Silva ACR**. 2004. Comparative genomics analyses of citrus-associated bacteria. *Annu Rev Phytopathol*. 42(1):163–184. https://doi.org/10.1146/annurev.phyto.42.040803.140310

**Newman MA**, **Dow JM**, **Daniels MJ**. 2001. Bacterial lipopolysaccharides and plant–pathogen interactions. *Eur J Plant Pathol*. 107:95–102.

**O'Connell A**, **An S-Q**, **McCarthy Y**, **Schulte F**, **Niehaus K**, **He Y-Q**, **Tang J-L**, **Ryan RP**, **Dow JM**. 2013. Proteomics analysis of the regulatory role of Rpf/DSF cell-to-cell signaling system in the virulence of *Xanthomonas campestris*. *Mol Plant Microbe Interact*. 26(10):1131–1137. https://doi.org/10.1094/MPMI-05-13-0155-R

**O'Grady EP**, **Nguyen DT**, **Weisskopf L**, **Eberl L**, **Sokol PA**. 2011. The *Burkholderia cenocepacia* LysR-type transcriptional regulator ShvR influences expression of quorum-sensing, protease, type II secretion, and *afc* genes. *J Bacteriol*. 193(1):163–176. https://doi.org/10.1128/JB.00852-10

**Onsando JM**. 1992. Black rot of crucifers. In: **Chaube HS**, **Singh US**, **Mukhopadyay AN**, **Kumar J**, editors. *Plant diseases of international importance. Diseases of vegetables and oil seed crops*. Englewood Cliffs (NJ): Prentice Hall. p. 243–252.

**Park H**, **Do E**, **Kim M**, **Park H-J**, **Lee J**, **Han S-W**. 2020. A LysR-type transcriptional regulator LcrX is involved in virulence, biofilm formation, swimming motility, siderophore secretion, and growth in sugar sources in *Xanthomonas axonopodis* pv. *glycines*. *Front Plant Sci*. 10:1657. https://doi.org/10.3389/fpls.2019.01657

**Parkinson N**, **Aritua V**, **Heeney J**, **Cowie C**, **Bew J**, **Stead D**. 2007. Phylogenetic analysis of *Xanthomonas* species by comparison of partial gyrase B gene sequences. *Int J Syst Evol Microbiol*. 57(12):2881–2887. https://doi.org/10.1099/ijs.0.65220-0

**Pielken P**, **Schimz K-L**, **Eggeling L**, **Sahm H**. 1987. Effect of methionine on xanthan formation by *Xanthomonas campestris*. *FEMS Microbiol Lett*. 44(1):27–31. https://doi.org/10.1111/j.1574-6968.1987.tb02236.x

**Pielken P**, **Schimz K-L**, **Eggeling L**, **Sahm H**. 1988. Glucose metabolism in *Xanthomonas campestris* and influence of methionine on the carbon flow. *Can J Microbiol*. 34(12):1333–1337. https://doi.org/10.1139/m88-234

**Qian G**, **Liu C**, **Wu G**, **Yin F**, **Zhao Y**, **Zhou Y**, **Zhang Y**, **Song Z**, **Fan J**, **Hu B**, **et al.** 2013. ASNB, regulated by diffusible signal factor and global regulator Clp, is involved in aspartate metabolism, resistance to oxidative stress and virulence in *Xanthomonas oryzae* pv. *oryzicola*. *Mol Plant Pathol*. 14(2):145–157. https://doi.org/10.1111/j.1364-3703.2012.00838.x

**Qian W**, **Han Z-J**, **He C**. 2008a. Two-component signal transduction systems of *Xanthomonas* spp.: a lesson from genomics. *Mol Plant Microbe Interact*. 21(2):151–161. https://doi.org/10.1094/MPMI-21-2-0151

**Qian W**, **Han Z-J**, **Tao J**, **He C**. 2008b. Genome-scale mutagenesis and phenotypic characterization of two-component signal transduction systems in *Xanthomonas campestris* pv. *campestris* ATCC 33913. *Mol Plant Microbe Interact*. 21(8):1128–1138. https://doi.org/10.1094/MPMI-21-8-1128

**Raboy V**. 2003. *myo*-Inositol-1,2,3,4,5,6-hexakisphosphate. *Phytochemistry*. 64(6):1033–1043. https://doi.org/10.1016/S0031-9422(03)00446-1

**Rashid MM**, **Ikawa Y**, **Tsuge S**. 2016. GamR, the LysR-type galactose metabolism regulator, regulates *hrp* gene expression via transcriptional activation of two key *hrp* regulators, HrpG and HrpX, in *Xanthomonas oryzae* pv. *oryzae*. *Appl Environ Microbiol*. 82(13):3947–3958. https://doi.org/10.1128/AEM.00513-16

**Richards GR**, **Vanderpool CK**. 2011. Molecular call and response: the physiology of bacterial small RNAs. *Biochim Biophys Acta Gene Regul Mech*. 1809(10):525–531. https://doi.org/10.1016/j.bbagrm.2011.07.013

**Rigano LA**, **Siciliano F**, **Enrique R**, **Sendín L**, **Filippone P**, **Torres PS**, **Qüesta J**, **Dow JM**, **Castagnaro AP**, **Vojnov AA**, **et al.** 2007. Biofilm formation, epiphytic fitness, and canker development in *Xanthomonas axonopodis* pv. *citri*. *Mol Plant Microbe Interact*. 20(10):1222–1230. https://doi.org/10.1094/MPMI-20-10-1222

**Rojas R**, **Nishidomi S**, **Nepomuceno R**, **Oshiro E**, **De Cassia Café Ferreira R**. 2013. Glutamate transport and xanthan gum production in the plant pathogen *Xanthomonas axonopodis* pv. *citri*. *World J Microbiol Biotechnol*. 29(11):2173–2180. https://doi.org/10.1007/s11274-013-1383-4

**Ruan Y-L**. 2014. Sucrose metabolism: gateway to diverse carbon use and sugar signaling. *Annu Rev Plant Biol*. 65(1):33–67. https://doi.org/10.1146/annurev-arplant-050213-040251

**Russell DA**, **Byrne GA**, **O'Connell EP**, **Boland CA**, **Meijer WG**. 2004. The LysR-type transcriptional regulator VirR is required for expression of the virulence gene *vapA* of *Rhodococcus equi* ATCC 33701. *J Bacteriol*. 186(17):5576–5584. https://doi.org/10.1128/JB.186.17.5576-5584.2004

**Russell WK**, **Park Z-Y**, **Russell DH**. 2001. Proteolysis in mixed organic-aqueous solvent systems: applications for peptide mass mapping using mass spectrometry. *Anal Chem*. 73(11):2682–2685. https://doi.org/10.1021/ac001332p

**Ryan RP**, **Fouhy Y**, **Lucey JF**, **Jiang B**, **He Y**, **Feng J**, **Tang J**, **Dow JM**. 2007. Cyclic di-GMP signalling in the virulence and environmental adaptation of *Xanthomonas campestris*. *Mol Microbiol*. 63(2):429–442. https://doi.org/10.1111/j.1365-2958.2006.05531.x

**Ryan RP**, **Vorhölter F-J**, **Potnis N**, **Jones JB**, **Van Sluys M-A**, **Bogdanove AJ**, **Dow JM**. 2011. Pathogenomics of *Xanthomonas*: understanding bacterium–plant interactions. *Nat Rev Microbiol*. 9(5):344–355. https://doi.org/10.1038/nrmicro2558

**Schäfer A**, **Tauch A**, **Jäger W**, **Kalinowski J**, **Thierbach G**, **Pühler A**. 1994. Small mobilizable multi-purpose cloning vectors derived from the *Escherichia coli* plasmids pK18 and pK19: selection of defined deletions in the chromosome of *Corynebacterium glutamicum*. *Gene*. 145(1):69–73. https://doi.org/10.1016/0378-1119(94)90324-7

**Schatschneider S**, **Persicke M**, **Watt SA**, **Hublik G**, **Pühler A**, **Niehaus K**, **Vorhölter F-J**. 2013. Establishment, in silico analysis, and experimental verification of a large-scale metabolic network of the xanthan producing *Xanthomonas campestris* pv. *campestris* strain B100. *J Biotechnol*. 167(2):123–134. https://doi.org/10.1016/j.jbiotec.2013.01.023

**Schindelin J**, **Arganda-Carreras I**, **Frise E**, **Kaynig V**, **Longair M**, **Pietzsch T**, **Preibisch S**, **Rueden C**, **Saalfeld S**, **Schmid B**, **et al.** 2012. Fiji: an open-source platform for biological-image analysis. *Nat Methods*. 9(7):676–682. https://doi.org/10.1038/nmeth.2019

**Schmidtke C**, **Abendroth U**, **Brock J**, **Serrania J**, **Becker A**, **Bonas U**. 2013. Small RNA sX13: a multifaceted regulator of virulence in the plant pathogen *Xanthomonas*. *PLoS Pathog*. 9(9):e1003626. https://doi.org/10.1371/journal.ppat.1003626

**Schulte F**, **Leßmeier L**, **Voss J**, **Ortseifen V**, **Vorhölter F-J**, **Niehaus K**. 2019. Regulatory associations between the metabolism of sulfur-containing amino acids and xanthan biosynthesis in *Xanthomonas campestris* pv. *campestris* B100. *FEMS Microbiol Lett*. 366(2):fnz005. https://doi.org/10.1093/femsle/fnz005

**Simm R**, **Morr M**, **Kader A**, **Nimtz M**, **Römling U**. 2004. GGDEF and EAL domains inversely regulate cyclic di-GMP levels and transition from sessility to motility. *Mol Microbiol*. 53(4):1123–1134. https://doi.org/10.1111/j.1365-2958.2004.04206.x

**Soares MR**, **Facincani AP**, **Ferreira RM**, **Moreira LM**, **De Oliveira JC**, **Ferro JA**, **Ferro MI**, **Meneghini R**, **Gozzo FC**. 2010. Proteome of the phytopathogen *Xanthomonas citri* subsp. *citri*: a global expression profile. *Proteome Sci*. 8(1):55. https://doi.org/10.1186/1477-5956-8-55

**Stock AM**, **Robinson VL**, **Goudreau PN**. 2000. Two-component signal transduction. *Annu Rev Biochem*. 69:183–215. https://doi.org/10.1146/annurev.biochem.69.1.183

**Storz G**, **Vogel J**, **Wassarman KM**. 2011. Regulation by small RNAs in bacteria: expanding frontiers. *Mol Cell*. 43(6):880–891. https://doi.org/10.1016/j.molcel.2011.08.022

**Tamir-Ariel D**, **Rosenberg T**, **Burdman S**. 2011. The *Xanthomonas campestris* pv. *vesicatoria citH* gene is expressed early in the infection process of tomato and is positively regulated by the TctDE two-component regulatory system. *Mol Plant Pathol*. 12(1):57–71. https://doi.org/10.1111/j.1364-3703.2010.00652.x

**Tang J-L**, **Liu Y-N**, **Barber CE**, **Dow JM**, **Wootton JC**, **Daniels MJ**. 1991. Genetic and molecular analysis of a cluster of *rpf* genes involved in positive regulation of synthesis of extracellular enzymes and polysaccharide in *Xanthomonas campestris* pathovar *campestris*. *Mol Gen Genet*. 226(3):409–417. https://doi.org/10.1007/BF00260653

**Timilsina S**, **Potnis N**, **Newberry EA**, **Liyanapathiranage P**, **Iruegas-Bocardo F**, **White FF**, **Goss EM**, **Jones JB**. 2020. *Xanthomonas* diversity, virulence and plant–pathogen interactions. *Nat Rev Mi-*

*crobiol*. 18(8):415–427. https://doi.org/10.1038/s41579-020-0361-8

**Tischler AD**, **Camilli A**. 2004. Cyclic diguanylate (c-di-GMP) regulates *Vibrio cholerae* biofilm formation. *Mol Microbiol*. 53(3):857–869. https://doi.org/10.1111/j.1365-2958.2004.04155.x

**Tyrrell R**, **Verschueren KH**, **Dodson EJ**, **Murshudov GN**, **Addy C**, **Wilkinson AJ**. 1997. The structure of the cofactor-binding fragment of the LysR family member, CysB: a familiar fold with a surprising subunit arrangement. *Structure*. 5(8):1017–1032. https://doi.org/10.1016/S0969-2126(97)00254-2

**Vicente JG**, **Holub EB**. 2013. *Xanthomonas campestris* pv. *campestris* (cause of black rot of crucifers) in the genomic era is still a worldwide threat to brassica crops. *Mol Plant Pathol*. 14(1):2–18. https://doi.org/10.1111/j.1364-3703.2012.00833.x

**Villanelo F**, **Ordenes A**, **Brunet J**, **Lagos R**, **Monasterio O**. 2011. A model for the *Escherichia coli* FtsB/FtsL/FtsQ cell division complex. *BMC Struct Biol*. 11(1):28. https://doi.org/10.1186/1472-6807-11-28

**Vojnov AA**, **Slater H**, **Daniels MJ**, **Dow JM**. 2001. Expression of the *gum* operon directing xanthan biosynthesis in *Xanthomonas campestris* and its regulation in planta. *Mol Plant Microbe Interact*. 14(6):768–774. https://doi.org/10.1094/MPMI.2001.14.6.768

**Vorhölter F-J**, **Niehaus K**, **Pühler A**. 2001. Lipopolysaccharide biosynthesis in *Xanthomonas campestris* pv. *campestris*: a cluster of 15 genes is involved in the biosynthesis of the LPS O-antigen and the LPS core. *Mol Gen Genomics*. 266(1):79–95. https://doi.org/10.1007/s004380100521

**Vorhölter F-J**, **Schneiker S**, **Goesmann A**, **Krause L**, **Bekel T**, **Kaiser O**, **Linke B**, **Patschkowski T**, **Rückert C**, **Schmid J**, **et al.** 2008. The genome of *Xanthomonas campestris* pv. *campestris* B100 and its use for the reconstruction of metabolic pathways involved in xanthan biosynthesis. *J Biotechnol*. 134(1–2):33–45. https://doi.org/10.1016/j.jbiotec.2007.12.013

**Wang F-F**, **Cheng S-T**, **Wu Y**, **Ren B-Z**, **Qian W**. 2017a. A bacterial receptor PcrK senses the plant hormone cytokinin to promote adaptation to oxidative stress. *Cell Rep*. 21(10):2940–2951. https://doi.org/10.1016/j.celrep.2017.11.017

**Wang H**, **Qian W-J**, **Mottaz HM**, **Clauss TRW**, **Anderson DJ**, **Moore RJ**, **Camp DG**, **Khan AH**, **Sforza DM**, **Pallavicini M**, **et al.** 2005. Development and evaluation of a micro- and nanoscale proteomic sample preparation method. *J Proteome Res*. 4(6):2397–2403. https://doi.org/10.1021/pr050160f

**Wang L**, **Pan Y**, **Yuan Z-H**, **Zhang H**, **Peng B-Y**, **Wang F-F**, **Qian W**. 2016. Two-component signaling system VgrRS directly senses extracytoplasmic and intracellular iron to control bacterial adaptation under iron-depleted stress. *PLoS Pathog*. 12(12):e1006133. https://doi.org/10.1371/journal.ppat.1006133

**Wang S**, **Sun S**, **Li Z**, **Zhang R**, **Xu J**. 2017b. Accurate de novo prediction of protein contact map by ultra-deep learning model. *PLoS Comput Biol*. 13(1):e1005324. https://doi.org/10.1371/journal.pcbi.1005324

**Wang S**, **Sun S**, **Xu J**. 2018. Analysis of deep learning methods for blind protein contact prediction in CASP12. *Proteins*. 86(S1):67–77. https://doi.org/10.1002/prot.25377

**Waterhouse A**, **Bertoni M**, **Bienert S**, **Studer G**, **Tauriello G**, **Gumienny R**, **Heer FT**, **de Beer TAP**, **Rempfer C**, **Bordoli L**, **et al.** 2018. SWISS-MODEL: homology modelling of protein structures and complexes. *Nucleic Acids Res*. 46(W1):W296–W303. https://doi.org/10.1093/nar/gky427

**Watt TF**, **Vucur M**, **Baumgarth B**, **Watt SA**, **Niehaus K**. 2009. Low molecular weight plant extract induces metabolic changes and the secretion of extracellular enzymes, but has a negative effect on the expression of the type III secretion system in *Xanthomonas campestris* pv. *campestris*. *J Biotechnol*. 140(1–2):59–67. https://doi.org/10.1016/j.jbiotec.2008.12.003

**Williams PH**. 1980. Black rot: a continuing threat to world crucifers. *Plant Dis*. 64:736–742. https://doi.org/10.1094/PD-64-736

**Xu J**, **McPartlon M**, **Li J**. 2021. Improved protein structure prediction by deep learning irrespective of co-evolution information. *Nat Mach Intell*. 3(7):601–609. https://doi.org/10.1038/s42256-021-00348-5

**Yun MH**, **Torres PS**, **Oirdi ME**, **Rigano LA**, **Gonzalez-Lamothe R**, **Marano MR**, **Castagnaro AP**, **Dankert MA**, **Bouarab K**, **Vojnov AA**. 2006. Xanthan induces plant susceptibility by suppressing callose deposition. *Plant Physiol*. 141(1):178–187. https://doi.org/10.1104/pp.105.074542

**Zhou J**, **Peng Z**, **Long J**, **Sosso D**, **Liu B**, **Eom J**, **Huang S**, **Liu S**, **Vera Cruz C**, **Frommer WB**, **et al.** 2015. Gene targeting by the TAL effector PthXo2 reveals cryptic resistance gene for bacterial blight of rice. *Plant J*. 82(4):632–643. https://doi.org/10.1111/tpj.12838